

**EFFECTS OF DEM RESOLUTION ON THE WEPP
RUNOFF AND EROSION PREDICTIONS:
A CASE STUDY OF FOREST AREAS IN NORTHERN IDAHO**

A Dissertation

Presented in Partial Fulfillment of the Requirements for the

Degree of Doctor of Philosophy

with a

Major in Geography

in the

College of Graduate Studies

University of Idaho

by

Xinxin (Jane) Zhang

August 2005

Major Professor: Kang-tsung Chang, Ph.D.

**AUTHORIZATION TO SUBMIT
DISSERTATION**

This dissertation of Xinxin (Jane) Zhang, submitted for the degree of Doctor of Philosophy with a major in Geography and titled “Effects of DEM Resolution on the WEPP Runoff and Erosion Predictions: A Case Study of Forest Areas in Northern Idaho”, has been reviewed in final form. Permission, as indicated by the signatures and dates given below, is now granted to submit final copies to the College of Graduate Studies for approval.

Major Professor _____ Date _____
Kang-tsung Chang

Committee
Members _____ Date _____
Joan Wu

_____ Date _____
William Elliot

_____ Date _____
Karen Humes

Department
Administrator _____ Date _____
Harley Johansen

Discipline’s
College Dean _____ Date _____
Judith T. Parrish

Final Approval and Acceptance by the College of Graduate Studies

_____ Date _____
Margrit von Braun

Abstract

DEMs (digital elevation models) can be used in a GIS (geographic information system) to represent topography and extract terrain features. DEMs vary in resolution and accuracy by the production method. The most widely used DEMs are the publicly accessible USGS (U.S. Geological Survey) NED (National Elevation Dataset) DEMs at 30-m and 10-m resolutions. There are other sources of DEMs with different resolutions and qualities, such as LIDAR (LIght Detection and Ranging) DEMs and SRTM (Shuttle Radar Topography Mission) DEMs. DEMs with different resolutions and sources can generate varied topographic and hydrologic features, which may in turn affect the runoff and sediment yield predictions in soil erosion models, such as the WEPP (Water Erosion Prediction Project) model.

This research project studies the effects of DEM resolutions and sources on 1) deriving topographic and hydrologic attributes, and 2) predicting watershed hydrology and water erosion using WEPP v2005. For two small forest watersheds located on Moscow Mountain in northern Idaho, six DEMs were prepared: LIDAR 30-m, 10-m, and 4-m DEMs, NED 30-m, 10-m DEMs, and SRTM 30-m DEM. These DEMs were used to calculate topographic and hydrologic parameters that served as inputs in WEPP. The model results were then compared with the runoff and sediment yield data observed at the watershed outlets.

This study has found that DEMs with different resolutions and sources can generate varied watershed shapes and structures, extract different hillslope and channel lengths and gradients, and produce significantly different sediment yield predictions in WEPP. In

general, as DEM resolution became finer, its accuracy was higher, the landscape was more precisely and accurately represented, and the sediment yield estimates approached closer to the observed values. Conversely, as DEM resolution became coarser, its accuracy was lower, and the sediment yield estimates departed from the observed values. The study has also found that LIDAR DEMs are potentially very useful tools for soil erosion modeling.

Acknowledgement

I extend my sincere appreciation to those individuals who helped me complete this project and my doctoral studies.

I thank my committee members, Drs. Chang, Wu, Elliot, and Humes, for their helpful guidance, comments, and suggestions during the course of this research project. I thank Dr. Karl Chang, my major professor, for his assistance with the LIDAR DEM collection, GIS analysis, and manuscript preparation. I thank Dr. Joan Wu for her encouragement and countless hours of help with the WEPP model. I thank Dr. William Elliot for his guidance and suggestions with the WEPP and GeoWEPP applications. I thank Dr. Karen Humes for her willingness to share her LIDAR data for the preliminary test runs at the early stage of my research.

I also thank Shuhui Dun for her technical assistance with the WEPP model simulations, Dr. Erin Brooks and Bill Dansart for their help in searching the raw field data of runoff and sediment yield, Dr. Andy Hudak and Jeff Evans for their assistance with the LIDAR data processing, and Sue Miller for her help with the GPS application. Their time and efforts in helping me within their areas of expertise were invaluable and I appreciate it.

I especially thank my husband Zheng for his patience, understanding and support during the completion of my academic endeavors.

To my husband, Zheng

Table of Contents

Title page.....	i
Authorization to submit dissertation.....	ii
Abstract.....	iii
Acknowledgements.....	v
Dedication.....	vi
Table of contents.....	vii
List of tables.....	ix
List of figures.....	x
Chapter 1. General introduction.....	1
Chapter 2. Effects of DEM resolution and source on soil erosion modeling: a case study using the WEPP model.....	4
1. Introduction.....	5
2. DEM sources and resolution.....	8
3. WEPP.....	12
4. Study area and data sets.....	15
5. Model runs and results.....	20
6. Statistical analysis of slope.....	26
7. Discussion.....	27
8. Summary.....	32
9. Acknowledgement.....	32
10. References.....	33

Chapter 3. Effects of DEM resolution on WEPP hydrologic and erosion prediction: a case study of two forest watersheds in northern Idaho.....	38
1. Introduction.....	39
2. Methodology.....	43
3. Results.....	51
4. Discussion.....	55
5. Summary and conclusions.....	57
6. Acknowledgement.....	59
7. References.....	67
Chapter 4. General conclusions and recommendations for further research.....	70
1. General conclusions.....	71
2. Recommendations for further research.....	72
3. References.....	75
Appendix A. Literature review.....	76
Appendix B. Statistical programs and outputs.....	100

List of Tables

Table 1.	Differences between NED and SRTM DEMs.....	9
Table 2.	Root mean square errors (RMSEs) of six DEMs from three sources at three resolutions.....	19
Table 3.	The GeoWEPP derived watershed areas, number of hillslopes, number of channels, and the WEPP predicted average annual runoff and sediment yield using different DEMs for Watershed 5.....	24
Table 4.	The GeoWEPP derived watershed areas, number of hillslopes, number of channels, and the WEPP predicted average annual runoff and sediment yield using different DEMs for Watershed 6.....	25
Table 5.	Slope statistics for Watershed 5.....	27
Table 6.	Slope statistics for Watershed 6.....	27
Table 7.	Major factors affecting the erosion simulation in Watershed 5.....	29
Table 8.	Major factors affecting the erosion simulation in Watershed 6.....	29
Table 9.	RMSEs (root mean square errors) of six DEMs from three sources at three resolutions.....	48
Table 10.	The GeoWEPP derived watershed areas, number of hillslopes, number of channels, and the WEPP predicted average annual runoff and sediment yield using different DEMs for Watershed 5.....	52
Table 11.	The GeoWEPP derived watershed areas, number of hillslopes, number of channels, and the WEPP predicted average annual runoff and sediment yield using different DEMs for Watershed 6.....	53

List of Figures

Figure 1.	Location map of the study area.....	17
Figure 2.	Hillshade image of the LIDAR 4-m DEM for the Paradise Creek subwatersheds.....	18
Figure 3.	Watershed 5 derived from the six DEMs.....	22
Figure 4.	Watershed 6 derived from the six DEMs.....	23
Figure 5.	Location map of the area of study.....	46
Figure 6.	Hillshade image derived from the LIDAR 4-m DEM for the Paradise Creek subwatersheds.....	47
Figure 7.	Yearly precipitation vs. 30-yr simulation of runoff events based on LIDAR 10-m DEM for Watershed 5.....	60
Figure 8.	Yearly precipitation vs. 30-yr simulation of sediment yield events based on LIDAR 10-m DEM for Watershed 5.....	61
Figure 9.	The first 16 months of the 30-yr simulation of sediment yield events based on LIDAR 10-m DEM for Watershed 5.....	62
Figure 10.	Yearly precipitation vs. 30-yr simulation of runoff events based on LIDAR 10-m DEM for Watershed 6.....	63
Figure 11.	Yearly precipitation vs. 30-yr simulation of sediment yield events based on LIDAR 10-m DEM for Watershed 6.....	64
Figure 12.	Annual average rainfall intensity vs. 30-yr simulation of runoff events based on LIDAR 10-m DEM for Watershed 5.....	65
Figure 13.	Annual average rainfall intensity vs. 30-yr simulation of runoff events based on LIDAR 10-m DEM for Watershed 6.....	66
Figure 14.	The D8 flow routing algorithm vs. the Dinf method.....	74
Figure 15.	Watershed discretization for WEPP application.....	95

Chapter 1
General introduction

DEMs (digital elevation models) can be used in a GIS (geographic information system) to represent topography and extract terrain features. DEMs vary in resolution and accuracy by the production method. The most widely used DEMs are the publicly accessible USGS (U.S. Geological Survey) NED (National Elevation Dataset) DEMs at 30-m and 10-m resolutions. There are other sources of DEMs with different resolutions and qualities, such as LIDAR (Light Detection and Ranging) DEMs and SRTM (Shuttle Radar Topography Mission) DEMs. DEMs with different resolutions and sources can generate varied topographic and hydrologic features, which may in turn affect the runoff and sediment yield predictions in soil erosion models, such as the WEPP (Water Erosion Prediction Project) model.

The purpose of this study is to discuss the effects of DEM resolutions and sources on 1) deriving topographic and hydrologic attributes, and 2) predicting watershed hydrology and water erosion using WEPP v2005. Six DEMs were prepared for two small forest watersheds located on Moscow Mountain in northern Idaho. They were LIDAR 30-m, 10-m, and 4-m DEMs, NED 30-m and 10-m DEMs, and SRTM 30-m DEM. These DEMs were used to calculate topographic and hydrologic parameters that served as inputs in WEPP. The model results were compared with the runoff and sediment yield data observed at the watershed outlets.

Three hypotheses were tested in the study:

Hypothesis 1: Effect of the DEM resolution. The resolution of the DEM has a significant effect on deriving topographic and hydrologic attributes of the watersheds, and in turn results in significantly different runoff and sediment yield predictions in WEPP. Finer-

resolution DEMs should generate better presentations of watershed shape and structure and closer predictions of runoff and sediment yield compared to the observed data.

Hypothesis 2: Effect of the DEM source. By holding the resolution constant, DEMs from different sources have significant effect on deriving topographic and hydrologic attributes, resulting in significantly different runoff and sediment yield predictions in WEPP. DEM sources with higher accuracy should generate better presentations of watershed shape and structure, and closer predictions of runoff and sediment yield compared to the observed data.

Hypothesis 3: Effect of the terrain. When using the same DEM, the characteristics of the watershed terrain have significant effect on WEPP predictions. It should be harder to extract realistic topographic and hydrologic attributes and to predict accurate runoff and sediment yield for complex terrain with large slope variations.

This dissertation is presented in four chapters, each emphasizing an aspect of the research project as a whole. Chapter 2 focuses mainly on the first purpose of the study. It presents the topographic and hydrologic attributes derived from the DEMs, compares features of the delineated watersheds, hillslopes and channels, and illustrates how those differences may affect soil erosion applications. Chapter 3 covers the second purpose of the study. It details the application of the WEPP model to the study area, examines the DEM performances in model predictions, and explores the long-term runoff and sediment yield simulations in the model. Chapter 4 contains the general conclusions of the research project. It confirms or rejects a hypothesis based on the results of the study, and provides recommendations for work to extend the research presented here.

Chapter 2

Effects of DEM resolution and source on soil erosion modeling:

a case study using the WEPP model

1. Introduction

Topography is a dominant control on earth surface processes. It directly moderates the flow of water over and through the earth's surface and in turn moderates soil wetness and soil erosion potential (Hutchinson 1996). Topography is often represented by digital elevation models (DEMs) in a geographic information system (GIS). The most common type of DEM is grid-based, with each grid point representing a cell of a certain size or resolution. DEMs vary in resolution and accuracy by the production method. Traditionally, a DEM is created from terrain data sampling, in which elevation points are measured at regularly spaced intervals (Lo and Yeung 2002). The interval determines the resolution of the DEM. For instance, U.S. Geological Survey (USGS) 30-m DEM data are stored as profiles, in which the spacing of the elevations along and between each profile is 30 meters. The most widely used DEMs are the publicly accessible USGS NED (National Elevation Dataset) DEMs at 30-m and 10-m resolutions and the SRTM (Shuttle Radar Topography Mission) DEMs at 30-m resolution.

How to automatically extract topographic and hydrologic features from DEMs has been studied for the past two decades (Mark 1983, O'Callaghan and Mark 1984, Band 1989a, 1989b, Jenson 1991, Moore et al. 1991, 1993, Florinsky 1998, Walker and Willgoose 1999, Band et al. 2000, Flanagan et al. 2000). DEMs can be used in a GIS to derive a wealth of information about topography, hydrological flow, and hydrological connectivity. Recent developments have demonstrated significant movements towards defining integrated land and water spatial entities in automated terrain analysis such as automatically delineating hillslopes and hillslope profiles for soil erosion modeling (Flanagan et al. 2000, MacMillan et al. 2003). The reliability of DEM-derived topographic and hydrologic parameters is a

function of both the accuracy and resolution of the input DEM (Garbrecht and Martz 2000).

A high-quality DEM input grid is the key element for ensuring reliable topographic and hydrologic parameter output grids (Van Remortel et al. 2001). However, the relatively coarse spatial resolution of most existing DEM data sets has limited the applicability of many of these efforts (MacMillan et al. 2003).

There are two ways of getting high-resolution DEMs. The first method creates new DEMs by decreasing the interval between sampled elevation points. The cost of creating such DEMs, however, increases exponentially for finer resolutions (Cochrane 1999). The requirements for computer systems to handle high-resolution DEMs also increase significantly due to the large amount of data contained. The second method interpolates fine DEMs from coarse DEMs. Mitasova et al. (1996), for example, used the regularized spline with tension method to interpolate a finer DEM from a 30-m DEM and reported that the interpolated surface yielded more accurate results of topographic analysis. The regularized spline with tension method is a spatial interpolation method that can produce a smooth surface by minimizing the overshoots and artificial pits in the original elevation data (Mitasova and Mitas 1993).

Not every one agrees with the use of spatial interpolation in creating fine DEMs. Zhang and Montgomery (1994) suggested that, since the spacing of the original data used to construct a DEM effectively limits the DEM's resolution, decreasing the grid size cannot increase the accuracy in representing the land surface but can potentially introduce interpolation errors. Desmet and Govers (1997) found that the conclusion made by Mitasova et al. (1996) was based on an erroneous and inappropriate implementation of the topographic factor for grid-based systems. Van Remortel et al. (2001) also argued that, although

smoothing algorithms such as the regularized spline with tension can correct some irregularities in a DEM, they can also result in unwanted smoothing or generalizing of other DEM cells that do not require any such correction and in some cases may result in gross over-extensions of slope lengths. However, because of the high cost associated with the traditional method for creating fine DEMs, spatial interpolation has become an option for generating fine DEMs, albeit a poor option conceptually.

Our understanding of the effect of DEM resolution on deriving topographic and hydrologic parameters has been limited due to the unavailability of fine DEMs (e.g., 4-m DEMs). Recent developments in LIght Detection and Ranging (LIDAR) technology suggest a new option for generating fine DEMs. LIDAR is a remote sensing technology that determines distance by measuring the time it takes for a laser beam to reflect back from a target to a detector (Turner 2000). LIDAR has become a new cost effective alternative to photogrammetry for creating high-quality, fine-resolution DEMs (Hill et al. 2000).

The purpose of this study is to discuss the effects of DEM resolutions on deriving topographic and hydrologic attributes. Since there are multiple sources of DEMs with same resolution but different accuracy (e.g., USGS 10-m DEM and LIDAR 10-m DEMs), DEMs from different sources will be discussed as well. The effects of these two aspects of DEMs are illustrated with reference to a soil erosion application in two small forest watersheds in northern Idaho. In the application, the primary interest is to evaluate the effect of using different DEMs as inputs to the WEPP (Water Erosion Prediction Project) model for sediment yield prediction.

This paper is organized into the following sections. Section 2 discusses different sources and spatial resolutions of DEMs. Section 3 starts with an overview of the WEPP

model and then discusses topographic elements and WEPP. Section 4 describes the study area and the DEM data sets for the study. Section 5 presents WEPP model runs and a statistical analysis of the differences between the predictions and the observed values. Section 6 includes statistical analyses of slopes derived from different DEMs. Section 7 discusses major findings of the study and their implications. Section 8 concludes the paper with a short summary.

2. DEM sources and resolution

2.1. DEM sources

Most GIS users in the United States use USGS DEMs, including currently available NED DEMs. Alternative sources for DEMs include SRTM DEMs and LIDAR DEMs. The SRTM is a joint project between the NASA (National Aeronautics and Space Administration) and NGA (National Geospatial-Intelligence Agency) to acquire earth images and map the world. Flown aboard the NASA Space Shuttle Endeavour (launched February 11-22, 2000), the SRTM successfully collected data over 80% of the Earth's land surface, for all areas between 60⁰ N and 56⁰ S latitude. These data have been processed to generate digital topographic maps and seamless DEMs in 1-arc-second (approximately 30-m) and 3-arc-second (approximately 90-m) spatial resolutions. Besides the global coverage, an advantage of the mission lies in the homogeneous quality of the DEMs (Rabus et al. 2003). Extensive DEM data from a single source as with SRTM DEMs is especially desirable because it is consistent and comparable across large areas.

Comparing with NED DEMs, many believe that SRTM DEMs are more accurate, especially over mining and quarry areas (USGS <http://ned.usgs.gov/Ned/faq.asp>). One major

difference between the two types of DEMs is that NED elevations are bare ground readings whereas SRTM elevations are canopy based. Other differences are listed in Table 1.

Table 1. Differences between NED and SRTM DEMs

	NED	SRTM
Resolution	1 Arc Second (~30-m resolution)	1 Arc Second (~30-m resolution)
Source Data	Maps / Aerial Photos	Radar Images
Source Resolution	10-m and 30-m	30-m
Source Dates	1925-1999	February, 2000
Surface Type	"Bare Earth"	"First Return"
Accuracy Specifications	7-m RMSE (root mean square error)	10-m RMSE

Source: USGS (<http://ned.usgs.gov/Ned/faq.asp>)

LIDAR is an active remote sensing technology that uses light to measure the range between a target and a sensor. Airborne LIDAR system is a measurement system in which pulses of light are emitted from an instrument mounted in an aircraft. The travel time of a pulse of light from the sensor to the reflecting surface and back is used to determine the range to the surface (Lee et al. 2003). The basic components of an airborne LIDAR system include a laser scanner mounted in an aircraft, GPS (global positioning system), and an Inertial Measurement Unit (IMU). Airborne LIDAR systems usually obtain measurements for the horizontal coordinates (x, y) and elevation (z) of the reflective objects scanned by the laser beneath the flight path. These measurements generate a three-dimensional cloud of points with irregular spacing (Zhang et al. 2003). LIDAR has become a cost effective alternative to photogrammetry for creating high-quality DEMs in a timely fashion (Hill et al. 2000). For typical commercial LIDAR systems, the vertical accuracy is 15 centimeters or

higher; the planimetric accuracy is 10 to 100 centimeters; and the post spacing is 0.5 to 2 meters (Flood 2001).

When a LIDAR sensor emits pulses to a forested area, the laser pulses pass through a forest canopy and reflect back to the sensor as layers of vegetation are hit. A single laser pulse can result in multiple returns as it passes through vegetation to the ground (Naesset 1997). The first surface hit, called the first return, is the top of the canopy, while the last surface hit is the ground or close to it. Points that hit in between the canopy and the ground are intermediate returns, which may represent branches and understory vegetation (Conner 2003). Raw LIDAR data must be processed and assembled into flight lines by return layers to distinguish between ground surface elevation, height of understory vegetation, and height of a forest (Lefsky et al. 2002). In order to generate a DEM from LIDAR points, measurements from nonground features such as vegetation, buildings, and vehicles must be identified and removed. A number of algorithms have been developed to remove nonground points from LIDAR datasets, such as the linear least-squares interpolation algorithm (Kraus and Pfeifer 1998), the slope-based filter algorithm (Vosselman 2000), and, more recently, the progressive morphological filter algorithm (Zhang et al. 2003).

Besides the overall measurement density and the accuracy of the laser scanner system, the quality of the LIDAR-extracted DEM depends on two other factors. The first factor is the post-processing algorithm that identifies and removes the nonground features (Wehr and Lohr 1999). There are two basic errors in classifying LIDAR measurements regardless of the filtering method used (Zhang et al. 2003). One is the commission error that classifies nonground points as ground measurements, and the other is the omission error that removes ground points mistakenly. The second factor is the spatial resolution used to convert

the irregularly spaced LIDAR points to the regularly spaced DEM. The transformation from points onto a grid can introduce a degree of error. Smith et al. (2003) have found that the most accurate DEM created from LIDAR points uses a similar spacing as the original points. If the grid spacing is too large, it may result in loss of data and higher errors at the boundaries of features.

2.2. DEM resolution

DEM resolution refers to the precision of the data. Traditionally, a DEM is created from terrain data sampling, in which elevation points are measured at regularly spaced intervals (Lo and Yeung 2002). The interval determines the resolution of the DEM. Numerous studies have shown that the accuracy of derived topographic and hydrologic attributes depends on the quality and resolution of the input DEM (Jenson and Domingue 1988, Jenson 1991, Chang and Tsai 1991, Florinsky 1998, Gao 1998). A large grid size means a more generalized terrain, which preserves only major relief features. Different DEM resolutions can therefore produce different local slope and aspect results (Gerrard and Robinson 1971, Fashi 1989). Generally, the accuracy of slope results decreases with the coarser DEM (Chang and Tsai 1991, Gao 1998). The disappearance of short, steep slopes and small topographic features tends to lengthen the flow path, thus increasing the size of catchment areas (Wilson and Gallant 2000). In other words, a coarse DEM may not be able to fully capture a complete, integrated drainage network (MacMillan et al. 2003).

It is logical to conclude that the choice of DEM resolution is important in minimizing representation errors of the terrain shape, which is measured by various primary terrain attributes computed from DEMs (Wilson and Gallant 2000). But determination of the

appropriate resolution of a DEM is usually a compromise between achieving fidelity to the true surface and respecting practical limits related to the density and accuracy of the source data. The spacing of the original data used to construct a DEM effectively limits the resolution of the DEM. Decreasing the grid size beyond the resolution of the original survey data does not increase the accuracy of the land surface representation of the DEM but can potentially introduce interpolation errors (Zhang and Montgomery 1994).

Although the research community is excited about the capability of extracting high-resolution DEM from LIDAR points, some researchers have found that the new option presents some unique problems for which solutions are still lacking or are insufficient (MacMillan et al. 2003). A fine-resolution DEM can sometimes pick out too much topographic detail, and can deflect stream flows from their natural courses by assumed or artifact barriers. So it seems inappropriate to claim that finer-resolution DEMs would invariably result in more accurate topographic and hydrologic parameters.

3. WEPP

3.1. Overview

The WEPP model is a physically-based, numerical process model used to predict erosion and sediment delivery on hillslopes and watersheds (Flanagan and Livingston, 1995). It was publicly released in 1995 for applications on agricultural lands, rangelands, and forests (Flanagan and Nearing, 1995). In the past decade, WEPP has been widely used to simulate soil erosion on hillslopes and at watershed level (Laflen et al. 1991, Laflen et al. 1997, Cochrane and Flanagan 1999, Renschler et al. 2000, Flanagan et al. 2002, Renschler and Harbor 2002). In order to improve the model's ability to predict erosion in a variety of

environmental conditions, the model has undergone continuous development. Forest lands, typified by steep slopes, and shallow, young, and coarse-grained soils, are highly different from common croplands and rangelands (Wu et al. 2000). Recent developments in WEPP v2005 have improved the model performance in forest watershed modeling so that it can adequately simulate forest watershed hydrology and erosion (Wu et al. 2000). The WEPP v2005 model was selected for this study.

Similar to other soil erosion models, one of the most demanding challenges in using the WEPP model is to determine the effect of topography on erosion, especially in topographically complex areas, such as mountain areas with large slope variations. Topography plays an important role in determining the amount of soils eroded by runoff water from hillslopes because the physical characteristics of a slope, such as slope gradient, length and shape, can determine the characteristics of flow across the surface (Foster 1982). Runoff water on steep slopes is more erosive, and can more easily transport detached sediment downslope. Long slope length allows a high volume of water to accumulate, resulting in an accelerated potential to erode. Concave slopes are less erosive than convex slopes because the slopes at the foot of the concave hill are less steep (Elliot and Ward 1995).

GIS has become an increasingly important and useful tool for preparing inputs to hydrologic and soil erosion modeling (Jenson, 1991; Moore et al., 1993; Hickey et al., 1994; Mitsova et al., 1996; Desmet and Govers, 1996, 1997; Tarboton, 1997; Cochrane and Flanagan, 1999; Walker and Willgoose, 1999; Gertner et al., 2002). WEPP is no exception. The Geo-spatial interface for WEPP (GeoWEPP) was developed to link the WEPP model with a GIS and to utilize DEM data to generate the necessary topographic inputs for erosion model simulations (Renschler, 2003). The interface uses TOPAZ (Garbrecht and Martz,

1997), a topography parameterization software package within the ArcView 3.x environment, to derive topographic input parameters for WEPP applications. TOPAZ can rectify depressions and flat surfaces in a DEM, identify hydrographic segmentations such as the channel network and corresponding drainage divides, and calculate topographic input parameters such as representative subcatchment parameters required by WEPP.

3.2. Topographic elements and WEPP

The WEPP model uses a slope profile to input topographic elements include slope length and gradient in its simulation. The slope profile can be automatically extracted from a DEM in GeoWEPP or manually generated by the user. A user can assign the overall profile length and slope values at user specified distances down the slope profile (Cochrane 1999). Distance downslope (x) is normalized to the slope length (L): $x^* = x / L$. The slope at a point is then processed and normalized to the average uniform slope gradient using the following equation to describe the slope shapes, namely convex, concave, or uniform:

$$S^* = a x^* + b \quad (1)$$

where S^* is the normalized slope (m m^{-1}), x^* is the normalized distance downslope (m m^{-1}), a and b are the calculated values describing shape of slope. If a is positive, S is a convex slope; if a is negative, S is a concave slope; and if a is zero, S is a uniform slope.

Micro topographic relief on hillslopes is also included in the simulation. In the hydrology component of the WEPP model, slope is an input for deriving the maximum depression storage that is defined as the portion of rainfall excess held in storage caused by micro-variations in topography. The maximum depression storage, S_d (m), is calculated from a relationship of random roughness and slope of the flow surface:

$$S_d = 0.112 r_r + 3.1 r_r^2 - 1.2 r_r S_o \quad (2)$$

where r_r is the random roughness (m), and S_o is the slope of flow surface (m m^{-1}).

In the erosion component of the WEPP model, topographic elements are used to calculate the shear stress acting on the soil, the friction coefficient, and the transport capacity of the flow. The shear stress acting on the soil, τ_{fe} (Pa), is calculated using the equation

$$\tau_{fe} = \gamma R \sin(\alpha) (f_s / f_t) \quad (3)$$

where γ is the specific weight of water ($\text{kg m}^{-2} \text{s}^{-2}$), α is the average slope angle for uniform segment, f_s is the friction factor for soil, and f_t is the total rill friction factor.

Under uniform flow conditions, the friction coefficient, f , is given as

$$f = 8gRS / V^2 \quad (4)$$

where g is acceleration due to gravity (m/s^2), R is hydraulic radius (m), S is average slope, and V is flow velocity (m/s).

The sediment transport capacity normalized to the transport capacity at the end of a uniform slope is

$$T_c^* = k_{tr} (a x^{*2} + b x^*) \quad (5)$$

where k_{tr} is the ratio of k_t , a transport coefficient ($\text{m}^{0.5} \text{s}^2 \text{kg}^{-0.5}$), to k_{tl} , the value of the transport coefficient for the uniform representative profile.

In short, topographic elements are deeply integrated into the hydrology and erosion components in the WEPP model. Therefore, it is important to use an accurate representation of the slope profile (Cochrane 1999).

4. Study area and data sets

4.1. Study area

The study area covers a portion of the headwater part of the Paradise Creek watershed in northern Idaho (Figure 1). The area consists of two small forest watersheds, located at the southwest boundary of Moscow Mountain. Forested steep slopes and moderately steep rolling hills characterize the area. The elevation varies from 880m to 1300m, and the slope ranges from 3% to 47%. The two small forest watersheds are named Watershed 5 and 6 corresponding to their respective monitoring sites (Figure 2). Monitoring site 5 is located upstream from monitoring site 6. Watershed 5 is therefore the upstream section of Watershed 6. Watershed 5 measures 106ha and Watershed 6 has 177ha.

4.2. DEM data sets

LIDAR data over the study area were acquired through the Horizon's Inc., a LIDAR service company. An algorithm was applied to generate DEMs from the LIDAR data, which are comprised of point data indicating the three-dimensional positions of object surfaces. The progressive morphological filter algorithm (Zhang et al. 2003) was selected for this purpose. This algorithm uses a progressive morphological filter to separate ground from nonground LIDAR measurements, such as vegetation in this case, by gradually increasing the window size of the filter and using an elevation difference threshold. Three LIDAR DEMs at 4-m, 10-m, and 30-m resolutions were generated using the algorithm. At the same time, three publicly accessible DEMs were collected for the study area: the USGS NED DEMs at 30-m and 10-m resolutions and the SRTM DEM at a 30-m resolution.

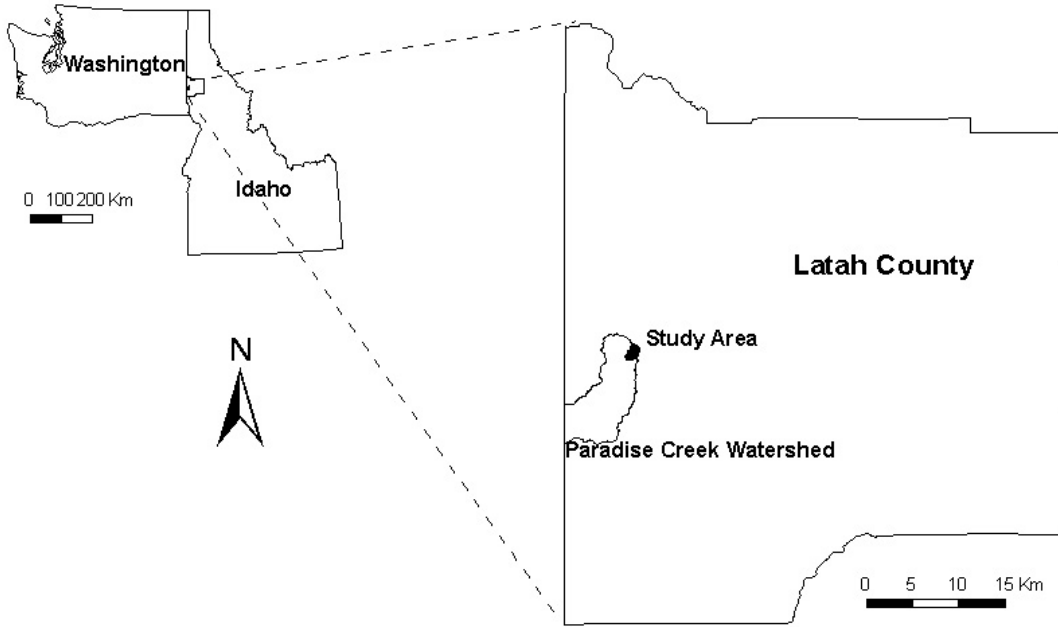


Figure 1. Location map of the study area.

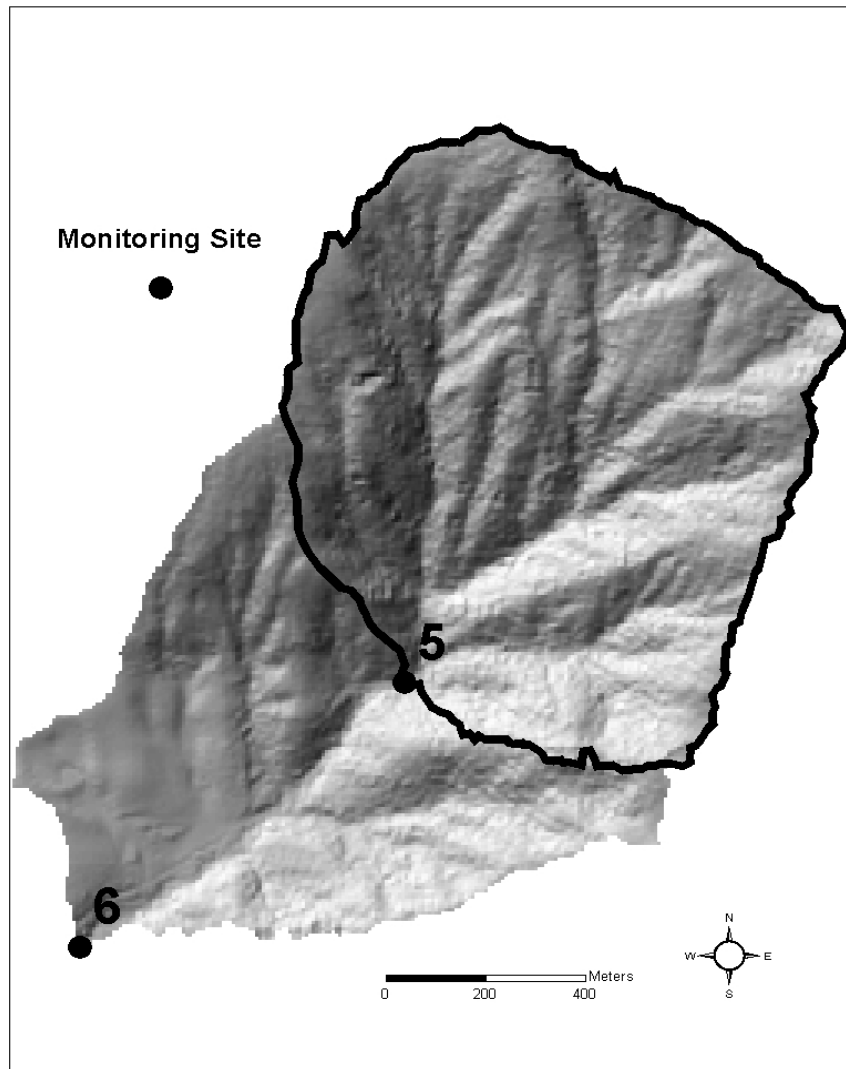


Figure 2. Hillshade image of the LIDAR 4-m DEM for the Paradise Creek subwatersheds. Monitoring site 5 and its corresponding contributing area, which is outlined by the black boundary, are located upstream of monitoring site 6 and its corresponding contributing area.

4.3. DEM accuracy assessment

The vertical accuracy of the six DEMs was assessed by using in-field GPS points in and around the study area. A total of 18 GPS points (assuming sufficient) were logged using Trimble TSC1 Asset Surveyor, and differentially corrected by the GPS Pathfinder Office software. The accuracy of the GPS system was tested to be 0.826m vertically and 0.704m horizontally. Based on the 18 GPS points, the RMSE (root mean square error) of each of the six DEMs for the vertical difference was calculated and listed in Table 2.

Table 2. Root mean square errors (RMSEs) of six DEMs from three sources at three resolutions.

	LIDAR DEM			NED DEM		SRTM DEM
Resolution (m)	30	10	4	30	10	30
RMSE (m)	5.733	1.511	1.244	3.865	3.012	5.652

The LIDAR 4-m and 10-m DEMs have the least RMSE, and the LIDAR and SRTM 30-m DEMs have the largest errors. The two NED DEMs, which do not differ much in accuracy, have the moderate level of RMSE.

4.4. Field observations

Water discharge and total suspended solid values for Watersheds 5 and 6 were measured at the monitoring sites on Paradise Creek every two weeks starting March 1999. For Watershed 5, the observation lasted till December 1999 with 18 records; for Watershed 6, the observation lasted till June 2002 with 65 records. Daily values of runoff and sediment yield were calculated from these records using linear interpolation method. Annual values were determined through integration, and their averages were calculated. For Watershed 5,

the average annual runoff is 138,940m³ and the sediment yield is 1.38t. For Watershed 6, the average annual runoff is 406,500m³ and the sediment yield is 4.55t.

5. Model runs and results

A WEPP model run requires the climate, management, soil, and topographic inputs. A 30-yr climate input was prepared based on the existing climate data observed at the closest weather station to the study area (City of Moscow University of Idaho station) for the period of 1973 to 2002. The management input was generated using the default file built in the WEPP model for a 20-year-old forest with 100 percent ground cover, which corresponds to the forest condition in the study area. The soil input was based on the default file built in the WEPP model for a 20-year-old forest with silt loam texture. Modifications were made in the soil input files about the bedrock hydraulic conductivity (3.6e-6mm/h) and the anisotropy ratio (50) values for hillslopes and channels to meet the requirement of the WEPP v2005 model. Also, the surface soil hydraulic conductivity (140mm/h) and the rock content values for hillslopes (40%) and channels (50%) were increased from the default values to adjust for the condition in the study area.

The topographic input, including both hillslope profiles and watershed channel files, were derived from each of the six prepared DEMs through the TOPAZ application in GeoWEPP. USGS DRG (digital raster graphic) maps provided the references to fix the derived channel networks and watershed structures. Figure 3 shows the derived Watershed 5 from each of the six DEMs and Figure 4 the derived Watershed 6.

The 30-m DEMs resulted in blocky watershed boundaries, hillslopes and stream networks for both watersheds. Watershed 5 derived from the SRTM 30-m DEM is perhaps

the poorest: almost all hillslopes in the watershed had straight-line boundaries, and the hillslope on the northeast corner even extended to the middle of the watershed area. The watersheds generated from the NED 10-m DEM had a few straight lines. The watersheds derived from the two LIDAR DEMs had no straight lines and improved the representation of topographic features dramatically. Besides having different shapes, these derived watersheds also have slightly different areas (Tables 3 and 4). The numbers of hillslopes and channels also varied in Tables 3 and 4.

The predicted average annual runoff and sediment yield for the two watersheds were obtained from the yearly values simulated by WEPP for the 30-year period. The predicted values were then compared with the observed data. The model predictions and the observed data are listed in Tables 3 and 4 for Watersheds 5 and 6, respectively. Compared to the observed data, all predictions overestimated both runoff and sediment yield in Watershed 5. But the differences among the runoff predictions (63% to 74% greater than the observed value) were much less than the sediment yield predictions (52.2% to 921.7% higher than the observed value). All three 30-m DEMs led to overestimations of sediment yields by more than 100% of the observed value. Among them, the SRTM DEM had the poorest result, followed by the LIDAR DEM and the NED DEM. The finer-resolution DEMs improved the model performance greatly. The LIDAR 10-m and 4-m DEMs and the NED 10-m DEM generated smaller overestimations of sediment yield, all under 100% off the observed value. The LIDAR 10-m DEM provided the closest predictions of runoff and sediment yield, followed by the LIDAR 4-m and NED 10-m DEMs.

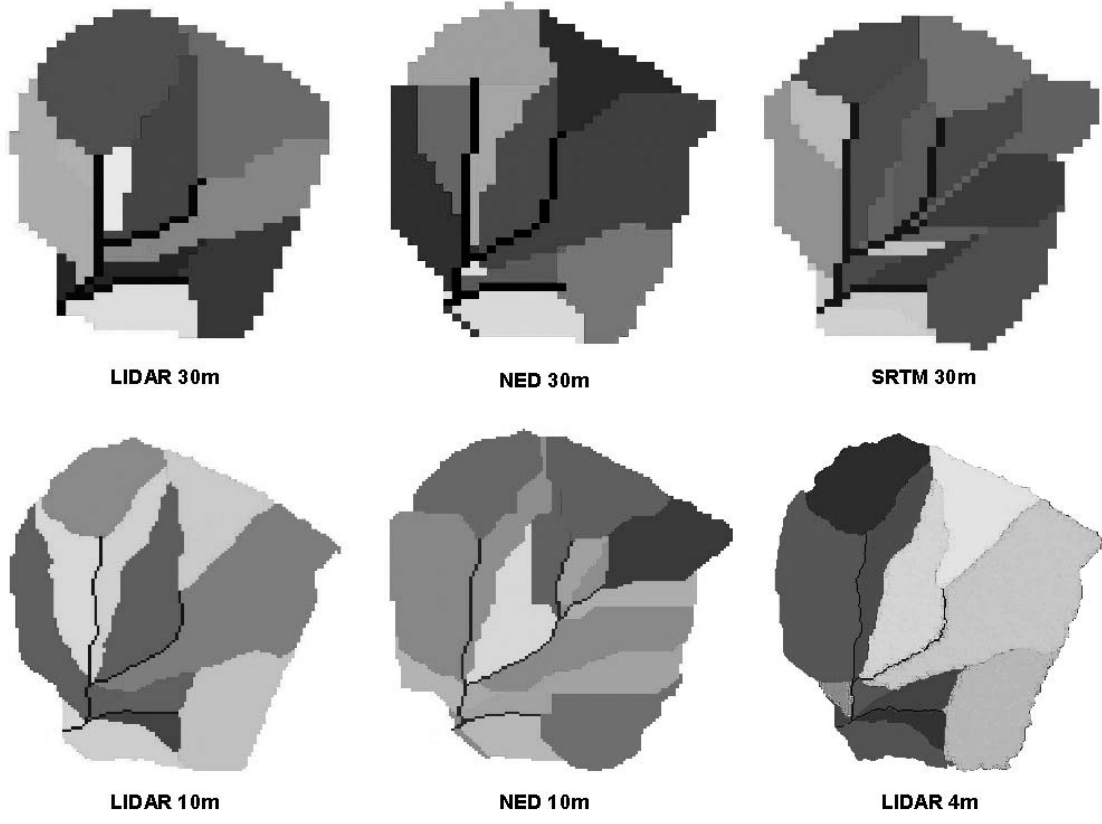


Figure 3. Watershed 5 derived from the six DEMs.

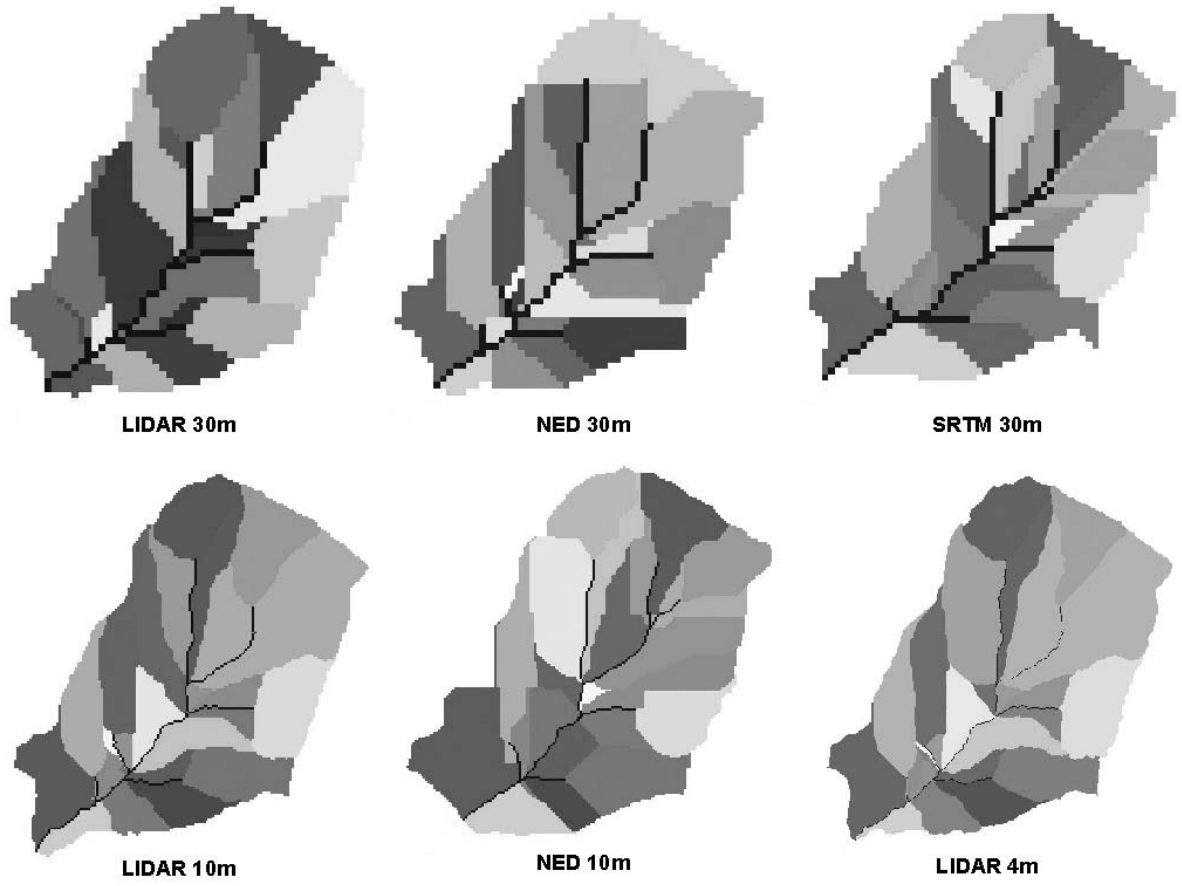


Figure 4. Watershed 6 derived from the six DEMs.

Table 3. The GeoWEPP derived watershed areas, number of hillslopes, number of channels, and the WEPP predicted average annual runoff and sediment yield using different DEMs for Watershed 5.^a

DEM	Area (ha)	Number of Hillslopes	Number of Channels	Runoff (m ³ /year)	Sediment Yield (t/year)
LIDAR 30-m	112.94	13	5	241118 (73.5) ^b	5.6 (305.8) ^b
NED 30-m	110.72	13	5	238844 (71.9)	4.0 (189.9)
SRTM 30-m	112.31	18	7	235007 (69.1)	14.1 (921.7)
LIDAR 10-m	106.06	13	5	226973 (63.4)	2.1 (52.2)
NED 10-m	111.66	18	7	232654 (67.5)	2.5 (81.2)
LIDAR 4-m	107.26	13	5	229098 (64.9)	2.2 (59.4)

a. GeoWEPP uses TOPAZ to derive the topographic parameters. As a comparison, the same parameters derived from ArcGIS 9® using LIDAR 4-m are: 106.43ha for the watershed area, 11 for the number of hillslopes, and 6 for the number of channels.

b. shown in parentheses are errors in percentage.

Results for Watershed 6 showed a different pattern of model predictions compared to those for Watershed 5 (Table 4). All six DEMs had underestimated runoff values. But only four of them had overestimated sediment yields. The predictions were much closer to the observed data than those for Watershed 5. The SRTM DEM still had the poorest predictions among the six DEMs for both runoff and sediment yield. Predictions from the other five DEMs were all less than 10% from the observed runoff and less than 40% from the observed sediment yield. Among the 30-m DEMs, the NED DEM and the LIDAR DEM provided very close predictions with the LIDAR DEM slightly better than the NED DEM in predicting runoff. The finer DEMs, LIDAR 10-m and 4-m and NED 10-m DEMs, did not improve the model performance as much as for Watershed 5. Still, they generated better predictions than the 30-m DEMs; the only exception was the NED 10-m DEM, which actually performed slightly worse than the NED 30-m DEM for the runoff prediction. The LIDAR 10-m DEM generated a very good prediction in runoff and the closest prediction in sediment yield. The

LIDAR 4-m DEM had the closest prediction in runoff and the second best prediction in sediment yield. Both LIDAR DEMs distinguished themselves from other DEMs by having very close predictions and consistent underestimation patterns for runoff and sediment yield. Overall, LIDAR 10-m DEM performed the best in predicting runoff and sediment yield for both Watersheds 5 and 6.

Table 4. The GeoWEPP derived watershed areas, number of hillslopes, number of channels, and the WEPP predicted average annual runoff and sediment yield using different DEMs for Watershed 6.^a

DEM	Area (ha)	Number of Hillslopes	Number of Channels	Runoff (m ³ /year)	Sediment Yield (t/year)
LIDAR 30-m	178.27	22	9	375795 (-7.6) ^b	6.2 (36.3) ^b
NED 30-m	176.14	27	11	374452 (-7.9)	6.2 (36.3)
SRTM 30-m	175.96	27	11	362753 (-10.8)	9.6 (111.0)
LIDAR 10-m	176.56	28	11	378949 (-6.8)	4.3 (-5.5)
NED 10-m	179.62	28	11	371966 (-8.5)	6.2 (36.3)
LIDAR 4-m	176.83	28	11	383005 (-5.8)	3.9 (-14.3)

a. GeoWEPP uses TOPAZ to derive the topographic parameters. As a comparison, the same parameters derived from ArcGIS 9® using LIDAR 4-m are: 176.60ha for the watershed area, 22 for the number of hillslopes, and 12 for the number of channels.

b. shown in parentheses are errors in percentage.

An analysis of variance (ANOVA) was carried out to test the differences between the model predictions and the observed values. The three dependent variables were the watershed area, runoff, and sediment yield. A significant level (α) of 0.05 was used to determine whether the differences in the dependent variable as indicated by the calculated F values, were significant.

The results showed that the differences among the watershed areas, as delineated by GeoWEPP and ArcGIS 9®, were not significant (F-value of 1.81, p-value of 0.2435). The observed runoff value and the model predicted runoff values from different DEMs did not

differ significantly ($F = 0.25$, $p = 0.9402$). However, the observed sediment yield and the model predictions from different DEMs were significantly different ($F = 5.23$, $p = 0.0320$).

6. Statistical analysis of slope

An analysis of the slope statistics was conducted for Watersheds 5 (Table 5) and 6 (Table 6). The results showed that, as the DEM resolution became finer, the average slope, standard deviation, and maximum slope values generally increased and the minimum slope value generally decreased. This finding is consistent with the observation that an averaging of elevations and slopes occur as the resolution is degraded (Gerrard and Robinson 1971, Fashi 1989, Chang and Tsai 1991, Florinsky 1998, Gao 1998). The terrain tends to be smoother as the DEM resolution becomes coarser. Using the LIDAR DEMs as an example, the average slope in Watershed 5 increased from 18.2, to 20.8, and to 21.5 degrees when the resolution was upgraded from 30-m, to 10-m, and to 4-m. Likewise, the average slope in Watershed 6 increased from 16.7, to 19.5, and to 20.2 degrees when the resolution was upgraded from 30-m, to 10-m, and to 4-m. By holding the resolution constant, DEMs from different sources produced varied slope statistics. For the 30-m DEMs, the NED DEM had the highest average slope and the maximum slope, followed by the LIDAR DEM and the SRTM DEM. For the 10-m DEMs, the NED DEM had a smaller average slope but a larger maximum slope than the LIDAR DEM. The LIDAR 4-m DEM produced the highest average slope, standard deviation, maximum slope, and the lowest minimum slope for both watersheds. Notice that the maximum slopes are identical for Watersheds 5 and 6 in Tables 5 and 6 because Watershed 5 is the upstream section of Watershed 6 and contains the steepest slopes in the area.

Table 5. Slope statistics for Watershed 5.

DEM	LIDAR 30-m	NED 30-m	SRTM 30-m	LIDAR 10-m	NED 10-m	LIDAR 4-m
Average Slope	18.17	18.93	16.85	20.79	20.37	21.46
Standard Deviation	5.70	5.90	4.98	5.78	6.18	6.71
Minimum Slope	0.26	1.38	1.38	0.28	1.04	0.00
Maximum Slope	32.98	33.29	29.14	37.56	41.56	47.33

Table 6. Slope statistics for Watershed 6.

DEM	LIDAR 30-m	NED 30-m	SRTM 30-m	LIDAR 10-m	NED 10-m	LIDAR 4-m
Average Slope	16.71	17.63	15.85	19.53	18.86	20.15
Standard Deviation	6.34	6.18	5.44	6.51	6.62	7.29
Minimum Slope	0.26	1.10	1.02	0.44	0.49	0.00
Maximum Slope	32.98	33.29	29.14	37.56	41.56	47.33

An ANOVA test was carried out to test if the slope values derived from the six DEMs were significantly different. A random sample of 30 points was generated in Watershed 6. Slope readings at the point locations were extracted from each of the slope grids derived from the six DEMs. A total of 180 slope readings were collected and used in the ANOVA test. The results showed that the differences among the slopes derived from the six DEMs were significant (F-value of 25.91, p-value less than 0.0001).

7. Discussion

The analysis of erosion predictions and the slope statistics revealed that DEMs that generated steeper average slopes resulted in less erosion. This may appear counter intuitive because it contradicts the general principle that steeper slopes have greater potential to erode. However, average slope gradient is only one of the many factors that affect erosion. Other factors include hillslope length, channel configuration and channel slope. Further examination of the GeoWEPP and WEPP results revealed that different DEMs resulted in

substantially different hillslope and channel systems, which in turn led to different erosion results (Tables 7 and 8). A combination of the aforementioned factors affected not only the gross sediment yield at the watershed outlet, but also the distribution of erosion between the hillslopes and the channels.

Using the SRTM 30-m DEM as an example, it simulated substantially more erosion than other DEMs. We can examine this phenomenon from several perspectives. First, the SRTM 30-m DEM delineated the longest average hillslope length in Watershed 5 and the second longest in Watershed 6. Both should accumulate more water and increase the erosion potential. Second, the SRTM 30-mDEM simulated the highest number of erosion-generating hillslopes for both watersheds, and most erosion occurred on hillslopes (77.3% to the total erosion for Watershed 5 and 82.6% for Watershed 6). Hillslope erosion was in fact the dominant form of erosion in the simulation. Third, the DEM delineated relatively steep average channel slope for both watersheds, which in turn should accelerate stream flow and channel erosion rate. The SRTM 30-m DEM simulated the second longest channel length in Watershed 5, but the second shortest in Watershed 6. This helped to explain why the erosion overestimation in Watershed 5 was greater than in Watershed 6.

In contrast, the LIDAR 4-m DEM simulated substantially less erosion than most other DEMs. It delineated the shortest average hillslope length in Watershed 6, and simulated the least number of erosion generating hillslopes for both watersheds. None of its erosion occurred on hillslope in Watershed 5 and only 2.6% in Watershed 6. Channel erosion was the dominant form the LIDAR 4-m DEM simulated. The DEM delineated the second flattest average channel slope in Watershed 5 and the flattest in Watershed 6. Flat channel slope should decelerate stream flow and decrease channel erosion.

Between the two extremes, other DEMs resulted in intermediate parameter values. The analysis showed that not a single parameter could fully explain the erosion phenomena. Every physical terrain feature contributed to the final simulation results in one aspect or another. This type of simulation is considered closer to reality than the type of simulation where only one or two factors determine the results. The relationship between the terrain features and the distribution of erosion, as shown in Tables 7 and 8, is therefore important to both the users and the developers of WEPP.

Table 7. Major factors affecting the erosion simulation in Watershed 5.

DEM	Total Erosion (t/yr)	Average Hillslope Length (m)	Number of Erosion Generating Hillslopes	Hillslope Erosion (t/yr)	Average Channel Slope (degree)	Total Channel Length (m)	Channel Erosion (t/yr)
LIDAR 30-m	5.6	228.1	1	2.7 (48.9) ^a	10.9	1933.7	2.9 (51.1) ^b
NED 30-m	4.0	207.3	1	1.3 (33.3)	13.7	2341.2	2.7 (66.8)
SRTM 30-m	14.1	238.1	2	10.9 (77.3)	14.6	2161.2	3.2 (22.7)
LIDAR 10-m	2.1	211.3	0	0.0 (0.0)	12.6	1786.4	2.1 (100.0)
NED 10-m	2.5	189.5	0	0.0 (0.0)	15.4	2150.2	2.5 (100.0)
LIDAR 4-m	2.2	212.9	0	0.0 (0.0)	11.4	1833.5	2.2 (100.0)

a. shown in parentheses are the ratios of hillslope erosion to total erosion

b. shown in parentheses are the ratios of channel erosion to total erosion

Table 8. Major factors affecting the erosion simulation in Watershed 6.

DEM	Total Erosion (t/yr)	Average Hillslope Length (m)	Number of Erosion Generating Hillslopes	Hillslope Erosion (t/yr)	Average Channel Slope (degree)	Total Channel Length (m)	Channel Erosion (t/yr)
LIDAR 30-m	6.2	237.9	2	2.8 (45.0) ^a	8.6	2965.2	3.4 (55.0) ^b
NED 30-m	6.2	204.7	3	1.6 (25.3)	11.1	3485.5	4.6 (74.7)
SRTM 30-m	9.6	237.7	5	7.9 (82.6)	10.9	3247.6	1.7 (17.4)
LIDAR 10-m	4.3	197.4	2	0.2 (5.3)	8.4	3390.8	4.1 (94.7)
NED 10-m	6.2	209.4	2	2.7 (43.5)	12.2	3330.8	3.5 (56.5)
LIDAR 4-m	3.9	187.7	1	0.1 (2.6)	7.9	3399.1	3.8 (97.4)

a. shown in parentheses are the ratios of hillslope erosion to total erosion

b. shown in parentheses are the ratios of channel erosion to total erosion

The study has found the LIDAR 10-m DEM may be a very good topographic input source. The watersheds delineated from it showed realistic boundary, structure, and hillslopes. The sediment yield predictions from it were the closest to the observed data. Overall, its performance was better than the LIDAR 4-m DEM in this study. This finding suggests that a 10-m DEM may be adequate to derive watershed topographic and hydrologic parameters, assuming that the DEM's accuracy is high enough. This finding is consistent with Zhang and Montgomery's (1994) claim that 10-m is the proper resolution and the rational compromise between increasing resolution and data volume for simulating geomorphic and hydrological processes.

The LIDAR 30-m DEM in this study revealed another aspect of LIDAR data important for soil erosion modeling. This DEM did not show any superiority to the NED 30-m DEM in terms of the accuracy, the quality of the delineated watersheds, or the sediment yield predictions. This suggests that large grid spacing in a LIDAR-extracted DEM can result in loss of data and high errors (Smith et al. 2003). In other words, a 30-m resolution may be too coarse to generate high-accuracy DEMs from very accurate raw LIDAR points.

The SRTM 30-m DEM may not be a good source for generating topographic and hydrologic attributes or for predicting sediment yields. Besides its coarse resolution, its elevations are canopy-based and are not appropriate for predicting erosion in small forested watersheds. The NED 10-m DEM was slightly more accurate than the NED 30-m DEM in this study. The 10-m DEM also generated slightly more realistic watersheds than the 30-m DEM. For sediment yield predictions, the two NED DEMs did not differ substantially, thus

suggesting they are of the same quality for deriving topographic and hydrologic attributes and erosion modeling.

Soil erosion predictions were better for the larger watershed than for the smaller watershed. The variation of the sediment yield predictions for the larger watershed was less than that for the smaller watershed. For instance, the sediment yield predictions from the LIDAR 30-m, NED 30-m, and NED10-m DEMs were identical for the larger watershed, but varied greatly for the smaller watershed. Topographically, the smaller watershed had steeper slopes and more complex terrain, which made the topographic input more important in the simulation. Selecting the appropriate DEM with proper accuracy and resolution is therefore critical for simulating hydrologic and erosion processes in mountainous areas with large slope variations and complex terrain.

Previous studies in WEPP applications have shown unsatisfactory simulations of forest watershed hydrology and erosion. Elliot et al. (1996) found that WEPP predicted only 50% of the observed runoff and 10 times more sediment yield than was observed in a harvested forest watershed. Koopman (2002) claimed that using 30-m DEMs, GeoWEPP over-predicted runoff by 10-50 times and under-predicted sediment yield by 50% than the observed values in small forest watersheds. Compared to these previous studies, this study has shown that WEPP v2005 can generate satisfactory predictions of runoff and sediment yield for forest watersheds by using the proper DEMs. The best predictions of runoff and sediment yield in this study were both under 6% off the observed values.

8. Summary

This study has shown that DEMs with different resolutions and sources can generate varied watershed shapes and structures, which can in turn result in significantly different sediment yield predictions in the WEPP model. Besides slope steepness, other DEM derived factors, such as hillslope length and channel length, can have significant effects on model simulation. This finding shows that DEM resolutions and sources have large impacts on deriving topographic and hydrologic attributes. The case study has illustrated how high-quality fine-resolution DEMs such as LIDAR 10-m DEM can assist in erosion modeling.

9. Acknowledgment

The authors thank Dr. William Elliot (Rock Mountain Research Station, USDA Forest Service) and Shuhui Dun (Department of Biological System Engineering Department, Washington State University) for their great suggestions and technical supports in model simulation. Dr. Erin Brooks (Department of Biological and Agricultural Engineering, University of Idaho) and Bill Dansart (Idaho Soil Conservation Commission) provided the raw field data of runoff and sediment yield. Sue Miller, Dr. Andy Hudak and Jeff Evans (Rocky Mountain Research Station, USDA Forest Service) helped in GPS application and LIDAR data processing. Their time and efforts are very much appreciated.

10. References

Band, L.E., 1989a, A terrain based watershed information system. *Hydrological Processes*, **3**, pp. 151-162.

Band, L.E., 1989b, Automated topographic and ecounit extraction from mountainous and forested watershed. *AI Application*, **3**, pp. 1-11.

Band, L.E., Tague, C.L., Brun, S.E., Tanenbaum, D.E., and Fernandes, R.A., 2000, Modeling watershed as spatial object hierarchies: structure and dynamics. *Transactions in GIS*, **4**(3), pp. 181-196.

Chang, K.T., and Tsai, B.W., 1991, The effect of DEM resolution on slope and aspect mapping. *Cartography and Geographic Information Systems*, **18**(1), pp. 69-77.

Cochrane, T.A., 1999, Methodologies for watershed modeling with GIS and DEMs for the parameterization of the WEPP model. Ph.D. thesis, Purdue University.

Cochrane, T.A., and Flanagan, D.C., 1999, Assessing water erosion in small watershed using WEPP with GIS and digital elevation models. *Journal of Soil and Water Conservation*, **54**(4), pp. 678-685.

Cochrane, T.A., and Flanagan, D.C., 2003, Representative hillslope methods for applying the WEPP model with DEMs and GIS. *Transactions of the ASAE*, **46**(4), pp. 1041-1049.

Conner, T.A., 2003, Using multi-return LIDAR data to measure forest stand characteristics in mixed coniferous forests of north central Idaho. Master's thesis, University of Idaho.

Desmet, P.J.J., and Govers, G, 1996, A GIS-procedure for automatically calculating the USLE LS factor on topographically complex landscape units. *Journal of Soil and Water Conservation*, **51**(5), pp. 427-433.

Desmet, P.J.J., and Govers, G, 1997, Comment on 'Modeling topographic potential for erosion and deposition using GIS'. *International Journal of Geographical Information Systems*, **11**(6), pp. 603-610.

Elliot, W.J., Luce, C.H., and Robichaud, P.R., 1996, Predicting sedimentation from timber harvest areas with the WEPP model. In *Proc. Sixth Federal Interagency Sedimentation Conf.*, Las Vegas, NEV, pp. 46-53.

Elliot, W.J., and Ward, A.D., 1995, Soil erosion and control practices. In *Environmental Hydrology*, A.D. Ward and W.J. Elliot (Eds.), pp. 177-204 (CRC Lewis Publishers, 1995)

Fahsi, A., 1989, The effect of spatial resolution of digital elevation model data on map characteristics. M. S. thesis, University of Idaho.

Flanagan, D.C., and Livingston, S.J., 1995, WEPP user summary, USDA-Water Erosion Prediction Project (WEPP). (W. Lafayette, IN: USDA-ARS National Soil Erosion Research Laboratory).

Flanagan, D.C., and Nearing, M.A., 1995, Technical documentation, USDA-Water erosion Prediction Project (WEPP). *NSERL Report*, **10**, (USDS-ARS National Soil Erosion Research Laboratory, West Lafayette, IN).

Flanagan, D.C., Renschler, C.S., and Cochrane, T.A., 2000, Application of the WEPP model with digital topographic information. In *Proceedings of the 4th international Conference on GIS and Environmental Modeling (GIS/EM4), Problems, Prospects and Research Needs*, 2-8 September 2000, Banff, Alta.

Flanagan, D.C., Renschler, C.S., Frankenberger, J.R., Cochrane, T.A., and Engel, B.A., 2002, Enhanced WEPP Model Applicability for Improved Erosion Prediction. In *ASA CSSA SSSA Pre-Meeting Workshop on Soil Erosion Assessment with the Process-Based WEPP Model*, Indianapolis, IN.

Flood, M., 2001, Laser altimetry: from science to commercial LIDAR mapping. *Photogrammetric Engineering and Remote Sensing*, **67**, pp. 1209-1217.

Florinsky, I.V., 1998, Accuracy of local topographic variables derived from digital elevation models. *International Journal of Geographical Information Systems*, **12**, pp. 47-61.

Foster, G., R., 1982, Modeling the erosion process. In *Hydrologic Modeling of Small Watersheds*, C.T. Haan, H.P. Johnson, D.L. Brakensiek (Eds.), pp. 297-380 (An ASAE Monograph Number 5 in a series published by ASAE).

Gao, J., 1998, Impact of sampling intervals on the reliability of topographic variables mapped from grid DEMs at a micro-scale. *International Journal of Geographical Information Systems*, **12**, pp. 875-890.

Garbrecht, J., and Martz, L.W., 1997, TOPAZ: Topographic Parameterization Software. El Reno, Okla.: USDA Agricultural Research Service, Grazinglands Research Laboratory. Available online at: <http://grl.ars.usda.gov/topaz/TOPAZ1.HTM>. (accessed 22 September 2004).

Garbrecht, J., and Martz, L.W., 2000, Digital elevation model issues in water resources modeling. In *Hydrologic and Hydraulic Modeling Support with Geographic Information Systems*. D. Maidment, and D. Djokic (Ed.), (Redland, CA: ESRI Press).

Gerrard, A.J.W., and Ronbinson, D.A., 1971, Variability in slope measurement: a discussion of the effects of different recording intervals and microrelief in slope studies. *Transactions, Institute of British Geographers*, **54**, pp. 45-54.

- Hickey, R., Smith, A., and Jankowski, P., 1994, Slope length calculations from a DEM within Arc/Info grid. *Computers, Environment and Urban Systems*, **18**(5), pp. 365-380.
- Hill, J.M., Graham, L.A., and Henry, R.J., 2000, Wide-area topographic mapping and applications using airborne Light Detection and Ranging (LIDAR) technology. *Photogrammetric Engineering & Remote Sensing*, **66**, pp. 908-914.
- Hutchinson, M.F., 1996, A locally adaptive approach to the interpolation of digital elevation models. *The Proceedings of Third International Conference/Workshop on Integrating GIS and Environmental Modeling*, January 21-26, 1996, Santa Fe, NM.
- Jenson, S.K., 1991, Application of hydrologic information automatically extracted from digital elevation models. *Hydrological Processes*, **5**, pp. 31-44.
- Jenson, S.K., and Domingue, J.O., 1988, Extracting topographic structure from digital elevation data for geographic information system analysis. *Photogrammetric Engineering and Remote Sensing*, **54**, pp. 1593-1600.
- Koopman, M., 2002, Geo-spatial prediction tools in forest management: Modeling post-burn hydrology of soil erosion in three western forests. MA thesis, Buffalo, State University of New York.
- Kraus, K., and Pfeifer, N., 1998, Determination of terrain models in wood areas with airborne laser scanner data. *ISPRS Journal of Photogrammetry and Remote Sensing*, **53**, pp. 193-203.
- Laflen, J.M., Lane, L.J., and Foster, G.R., 1991, WEPP: A New Generation of Erosion Prediction Technology. *Journal of Soil and Water Conservation*, **46**, pp. 34-38.
- Laflen, J.M., Elliot, W.J., Flanagan, D.C., Meyer, C.R., and Nearing, M.A., 1997, WEPP – Predicting water erosion using a process-based model. *Journal of Soil and Water Conservation*, **52**(2), pp. 96-102.
- Lee, H.S., and Younan, N.H., 2003, DTM extraction of LIDAR returns via adaptive processing. *IEEE Transaction on Geoscience and Remote Sensing*, **41**(9), pp. 2063-2069.
- Lefsky, M.A., Cohen, W.B., Parker, G.G., and Harding, D.D., 2002, LIDAR remote sensing for ecosystem studies. *Bioscience*, **52**(1), pp. 19-30.
- Lo, C.P., and Yeung, A.K.W., 2002, In *Concepts and Techniques of Geographic Information Systems*, (Prentice Hall Inc).

- MacMillan, R.A., Martin, T.C., Earle, T.J., and McNabb, D.H., 2003, Automated Analysis and Classification of Landforms Using High-Resolution Digital Elevation Data: Application and Issues. *Can. J. Remote Sensing*, **29**(5), pp. 592-606.
- Mark, D.M., 1983, Automated detection of drainage networks for digital elevation models, *Proceedings of Auto-Carto*, **6**(2), Ottawa, Ontario, Canada, pp. 288-298.
- Mitasova, H., and Mitas, L., 1993, Interpolation by regularized spline with tension: I. Theory and implementation. *Mathematical Geology*, **25**(6), pp. 641-655.
- Moore, I.D., Grayson, R.B., and Ladson, A.R., 1991, Digital terrain modeling: a review of hydrological, geomorphological, and biological applications. *Hydrological Processes*, **5**, pp. 3-30.
- Moore, I.D., Turner A.K., Wilson, J.P., Jenson, S.K., and Band, L.E., 1993, GIS and land-surface-subsurface process modelling. In *Environmental Modeling with GIS*, M.F. Goodchild, B.O. Park, and L.T. Styært (Ed.), pp. 213–230 (Oxford, UK: Oxford University Press).
- Naesset, E., 1997, Estimating timber volume of forest stands using airborne laser scanner data. *Remote Sensing Environment*, **61**, pp. 246-253.
- O’Callaghan, J.F., and Mark, D.M., 1984, The extraction of drainage networks from digital elevation data. *Computer Vision, Graphics and Image Processing*, **28**, pp. 328-344.
- Rabus, B., Eineder, M., Roth, A., and Bamler, R., 2003, The shuttle radar topography mission - a new class of digital elevation models acquired by spaceborne radar. *ISPRS Journal of Photogrammetry and Remote Sensing*, **57**(4), pp. 241-262.
- Renschler, C.S., Engel, B.A., and Flanagan, D.C., 2000, Strategies for implementing a multi-scale assessment tool for natural resource management: a geographical information science perspective. *The 4th International Conference on Integrating GIS and Environmental Modeling (GIS/EM4): Problems, Prospects, and Research Needs*, 2-8 September 2000, Banff, Alberta, Canada.
- Renschler, C.S., and Harbor, J., 2002, Soil erosion assessment tools from point to regional scales – the role of geomorphologists in land management research and implementation. *Geomorphology*, **47**, pp.189-209.
- Renschler, C.S., 2003, Designing geo-spatial interfaces to scale process models: the GeoWEPP approach. *Hydrological Processes*, **17**, pp. 1005-1017.
- Smith, S.L., Holland, D.A., and Longley, P.A., 2003, The effect of changing grid size in the creation of laser scanner digital surface models. *Proceedings of the 7th International*

Conference on GeoComputation, 8 - 10 September 2003, University of Southampton, United Kingdom

Tarboton, D.G., 1997, A new method for the determination of flow directions and upslope areas in grid digital elevation models. *Water Resources Research*, **33**(2), pp. 309-319.

Turner, A.K., 2000, LIDAR provides better DEM data. *GEOWorld*, **13**(11), pp. 30-31.

USGS <http://ned.usgs.gov/Ned/faq.asp> USGS NED Frequently Asked Questions. (accessed 15 March 2005).

Van Remortel, R., Hamilton, M., and Hickey, R., 2001, Estimating the LS factor for RUSLE through iterative slope length processing of digital elevation data within ArcInfo Grid. *Cartography*, **30**(1), pp. 27-35.

Vosselman, G., 2000, Slope based filtering of laser altimetry data. *International Archive of Photogrammetry and Remote Sensing B4*, **33**, pp. 958–964.

Walker, J.P., and Willgoose, G.R., 1999, On the effect of digital elevation model accuracy on hydrology and geomorphology. *Water Resources Research*, **35**(7), pp. 2259-2268.

Wehr, A., and Lohr, U., 1999, Airborne laser scanning - an introduction and overview. *ISPRS Journal of Photogrammetry & Remote Sensing*, **54**, pp. 68–82.

Wilson, J.P., and Gallant, J.C., 2000, *Terrain Analysis: Principles and Applications*. (John Wiley & Sons, Inc).

Wu, J.Q., Xu, A.C., Elliot, and W.J., 2000, Adapting WEPP for forest watershed erosion modeling. *Paper No. 002069. The 2000 International ASAE Meeting*, 9-12 July, Milwaukee, WI. St. Joseph, MI.

Zhang, K., Chen, S.C., Whitman, D., Shyu, M.L., Yan, J., and Zhang, C., 2003, A progressive morphological filter for removing nonground measurement from airborne LIDAR data. *IEEE Transaction on Geoscience and Remote Sensing*, **41**(4), pp. 872-882.

Zhang, W.H., and Montgomery, D.R., 1994, Digital elevation model grid size, landscape representation, and hydrologic simulations. *Water Resources Research* **30**(4), pp. 1019-1028.

Chapter 3

Effects of DEM resolution on WEPP hydrologic and erosion prediction:

a case study of two forest watersheds in northern Idaho

1. Introduction

In undisturbed forests, soils are covered by vegetation and litter. The soils typically have high infiltration rates because of the extensive root system and high organic content. Consequently, overland flow in forested areas is minimal, resulting in low water erosion and sediment yield. The soils in forested areas usually are shallow and coarse-grained, underlain by less permeable bedrock. They have high hydrologic conductivity developed due to predominant lateral flow over long time period. The subsurface runoff (lateral flow) often counts for the major contribution to stream flow in forest areas. Subsurface flow is much less likely than overland flow to cause erosion (Luce 1995). Overall, the water erosion rates in forestlands are typically low.

However, it is easy to increase sediment yields dramatically with careless management (Luce 1995). Forest stream pollution by excessive sedimentation can be one of the main concerns in forest management and water quality control. There is a need to accurately simulate and predict sedimentation from hillslopes to streams at the watershed scale in forested areas.

The Water Erosion Prediction Project (WEPP) is a physically-based, numerical process model used to predict erosion and sediment delivery on hillslopes and watersheds (Flanagan and Livingston 1995). WEPP uses climate, topography, soil, and management inputs to simulate infiltration, water balance, plant growth, residue decomposition, surface runoff, erosion, and sediment delivery over a range of time scales, including storm events, monthly, yearly, or long-term annual average. WEPP was publicly released in 1995 and has undergone continuous development since then. Recent developments in WEPP v2005, have improved the model performance in forest watershed modeling. The WEPP model can

adequately simulate forest watershed hydrology and erosion, and can solve the problem of underestimating lateral flows and subsequently underestimating channel erosion in forest watersheds in the original WEPP model (Wu et al. 2000). To do that, the revised WEPP model (v2005) has a bedrock layer that has a hydraulic conductivity value near zero in the soil profile to limit the amount of water lost to deep percolation. This revision model matches the forest conditions where soils often have low permeable bedrock underneath. Secondly, it includes the concept of the anisotropy ratio to the soil profile. An anisotropy ratio greater than 1 represents the physical nature of the soil on forested slopes that it has a much higher horizontal saturated hydraulic conductivity than in vertical direction due to the underlying bedrock and sloping terrain. The addition of this layer improves the forest hydrologic simulation by increasing the amount of subsurface lateral flow reaching the bottom of the hillslope. The revised WEPP model adds the properly simulated subsurface lateral flow to the overland flow and routes it to the watershed outlet.

Geographic information system (GIS) has become an increasingly important and useful tool for preparing inputs to hydrologic and soil erosion modeling (Mitasova et al. 1996, Desmet and Govers 1996). The Geo-spatial interface for WEPP (GeoWEPP) was developed to link the WEPP model with a GIS and to utilize digital elevation model (DEM) to generate the necessary topographic inputs for erosion model simulations (Renschler 2003). The interface uses TOPAZ (Garbrecht and Martz 1997), a topography parameterization software package within the ArcView 3.x environment, to derive topographic input parameters for WEPP applications. Many existing GeoWEPP applications have been based on the 30-m USGS DEMs (Renschler and Harbor 2002)

The most common type of DEM is grid-based, with each grid point representing a cell of a certain size or resolution. DEMs vary in resolution and accuracy by the production method. The most widely used DEMs are the publicly accessible NED (National Elevation Dataset) DEMs at 30-m and 10-m resolutions and the SRTM (Shuttle Radar Topography Mission) DEMs at 30-m resolution. The National Elevation Dataset is a raster product assembled by the USGS. In addition to the standard 1-arc-second resolution (approximately 30-m), NED data for a portion of the United States are available in 1/3-arc-second resolution (approximately 10-m). The SRTM is a joint project between NASA (National Aeronautics and Space Administration) and NGA (National Geospatial-Intelligence Agency) to acquire earth images. Flown aboard the NASA Space Shuttle Endeavour (launched February 11-22, 2000), the SRTM successfully collected data over 80% of the Earth's land surface. These data have been processed to generate digital topographic maps and seamless DEMs in 1-arc-second (approximately 30-m) and 3-arc-second (approximately 90-m) spatial resolutions. The accuracy of the above DEMs varies. DEM accuracy is normally expressed as the root mean square error (RMSE), which represents the difference between the elevation values in the DEM and the true values of elevation on the terrain. The true values can come from benchmarks, independent field measurements or more accurate data sources. For the 30-m NED and SRTM DEMs, their RMSEs are approximately 7-m and 10-m, respectively.

Numerous studies have shown that the reliability of the derived topographic and hydrologic attributes depends on the resolution and accuracy of the input DEM (Jenson and Domingue 1988, Jenson 1991, Chang and Tsai 1991, Florinsky 1998, Gao 1998). A large grid size means a more generalized terrain, which preserves only major relief features. Different DEM resolutions can therefore produce different local slope and aspect results

(Gerrard and Robinson 1971, Fashi 1989). Subsequently DEM accuracy and resolution can influence the result of soil erosion models (Mitasova et al. 1996, Gertner et al. 2002). In the case of WEPP, DEM resolution and accuracy can influence hillslope length, channel configuration and channel slope in a watershed, which can affect not only the gross sediment yield at the watershed outlet, but also the distribution of erosion between the hillslopes and channels. The relatively coarse spatial resolution and low accuracy level of most existing DEM datasets has limited the model's simulation capability.

The cost of creating DEMs increases exponentially for finer resolutions (Cochrane 1999). Because of their limited availability, fine DEMs have rarely been used on soil erosion modeling. A gap therefore exists in the literature for a systematic study of the effects of DEM resolution on soil erosion in forested areas.

Recent developments in LIght Detection and Ranging (LIDAR) technology provide a new option for generating fine and high-quality DEMs. LIDAR is a remote sensing technology that determines distance by measuring the time it takes for a laser beam to reflect back from a target to a detector (Turner 2000). The airborne LIDAR system is a measurement system in which pulses of light are emitted from an instrument mounted in an aircraft. The travel time of a pulse of light from the sensor to the reflecting surface and back is used to determine the range to the surface (Lee and Younan 2003). Airborne LIDAR systems usually obtain measurements for the horizontal coordinates (x, y) and elevation (z) of the reflective objects scanned by the laser beneath the flight path. These measurements generate a three-dimensional cloud of points with irregular spacing (Zhang et al. 2003). Since LIDAR data are not comprised of pixels with a spatial dimension, but rather of point data indicating the three-dimensional positions of object surfaces, an algorithm must be applied to

generate DEMs from LIDAR point data. In order to generate DEMs from LIDAR points, measurements from nonground features such as vegetation, buildings, and vehicles must be identified and removed. A number of algorithms have been developed to remove nonground points from LIDAR datasets, such as the linear least-squares interpolation algorithm (Kraus and Pfeifer 1998), the slope-based filter algorithm (Vosselman 2000), and, more recently, the progressive morphological filter algorithm (Zhang et al. 2003). LIDAR has become a new cost effective alternative to photogrammetry for creating high-quality, fine-resolution DEMs (Hill et al. 2000). Thus, in addition to the publicly accessible DEMs, LIDAR DEMs have become a new source of DEMs. Using LIDAR-generated high-resolution DEMs in erosion models provides a promising path to improve model performance.

The purpose of this study is threefold: to apply WEPP v2005 for hydrological and erosion simulation under a forest setting; to evaluate the effects of DEM resolution and accuracy on watershed hydrology and water erosion prediction at watershed scale; and to examine the long-term runoff and sediment yield patterns in the watersheds simulated by the model. Runoff and sediment yield in two small forest watersheds located on Moscow Mountain in northern Idaho were collected and processed. A total of six DEMs from three sources at three resolutions were then used to calculate topographic parameters as inputs to the WEPP model. WEPP hydrologic and erosion results from using the six different DEMs were compared with the observed data.

2. Methodology

2.1. Study area

The study area consists of two small forest watersheds, located at the southwest boundary of Moscow Mountain in Latah County in northern Idaho (Figure 5). They cover a portion of the headwater area of the Paradise Creek watershed, which is part of the Palouse River hydrologic basin. Forested steep slopes and moderately steep rolling hills characterize the area. The elevation varies from 880m to 1300m, and the slope ranges from 3% to 47%. The two small forest watersheds are named 5 and 6 corresponding to their respective monitoring sites (Figure 6). Monitoring site 5 is located upstream from monitoring site 6. Watershed 5 is therefore the upstream section of Watershed 6, measuring 106ha and 177ha, respectively.

According to the Paradise Creek TMDL report made by the Idaho Division of Environmental Quality (1997), soils in the study area fall into the silt loam category. They are well-drained soils formed in volcanic ash, loess and granitic residuum. The bedrock of the watershed consists predominantly of granite. Due to the soil characteristics and the steep topography, runoff in the study area is rapid and the hazard for water erosion is high.

Vegetation in the study area is coniferous forests, mainly Douglas fir and ponderosa pine. Much of the forested land in Paradise Creek watershed had been subject to timber harvest. Since the landowner carried out the healthy environmental practices in 1994, there has been little timber harvesting or related road building. Recreational activities, such as hunting, hiking, mountain biking, recreational vehicle riding, and cross-country skiing, however, take place in the headwater area, which likely contribute to erosion and sedimentation of streams.

Precipitation within the Paradise Creek watershed falls mainly in winter season (Nov. – Feb.), as either snow or a combination of rain and snow. During the spring months, the

winter snowpack melts and causes prolonged high flows. Rainfall coinciding with snowmelt and rainfall onto frozen soils typically cause peak flows within the watershed. In the headwaters, Paradise Creek is intermittent, running for several months from the spring thaw until May or June. In the summer, flow stops, reducing the stream to a dry creek bed.

2.2. DEM preparation and accuracy assessment

LIDAR data over the study area were acquired through the Horizon's Inc., a LIDAR service company. The progressive morphological filter algorithm (Zhang et al. 2003) was selected to generate DEMs. This algorithm uses a progressive morphological filter to separate ground from nonground LIDAR measurements, such as vegetation in this case, by gradually increasing the window size of the filter and using an elevation difference threshold. Three LIDAR DEMs at 4-m, 10-m, and 30-m resolutions were generated using the algorithm.

Three publicly accessible DEMs for the study area were downloaded from the official USGS website at <http://seamless.usgs.gov>. They were the NED DEMs at 30-m and 10-m resolutions, and the SRTM DEM at a 30-m resolution. Thus, a total of six DEMs were prepared for the study area.

The vertical accuracy of the six DEMs was assessed using in-field GPS points in and around the study area. A total of 18 GPS points (assumed sufficient) were logged using Trimble TSC1 Asset Surveyor, and differentially corrected by the GPS Pathfinder Office software. The accuracy of the GPS system was tested to be 0.826m vertically and 0.704m horizontally. Based on the 18 GPS points, the RMSE of each of the six DEMs for the vertical difference was calculated and listed in Table 9.

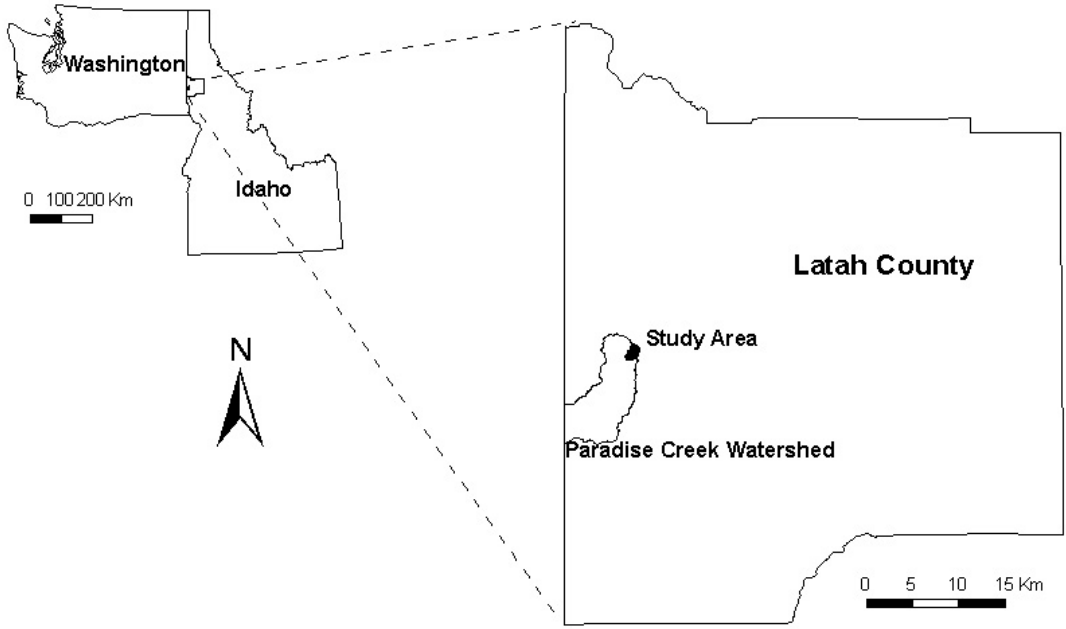


Figure 5. Location map of the area of study.

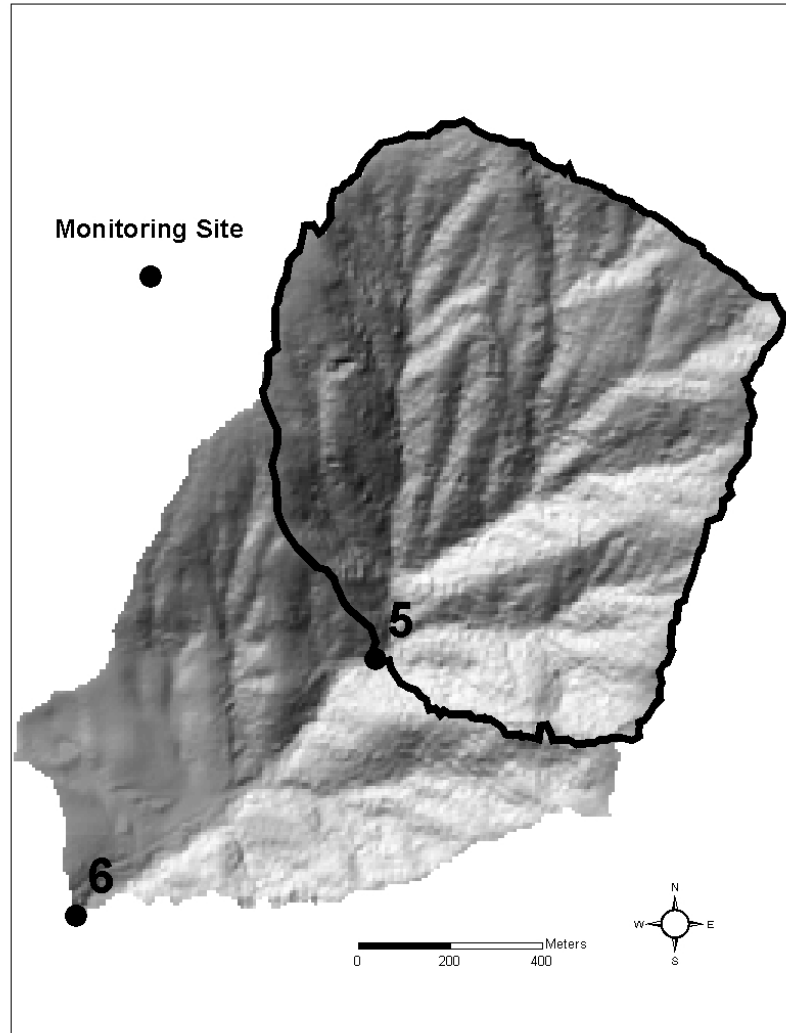


Figure 6. Hillshade image derived from the LIDAR 4-m DEM for the Paradise Creek subwatersheds. Monitoring site 5 and its corresponding contributing area, which is outlined by the black boundary, are located upstream of monitoring site 6 and its corresponding contributing area.

Table 9. RMSEs (root mean square errors) of six DEMs from three sources at three resolutions

	LIDAR DEM			NED DEM		SRTM DEM
Resolution (m)	30	10	4	30	10	30
RMSE (m)	5.733	1.511	1.244	3.865	3.012	5.652

The LIDAR 4-m and 10-m DEMs have the least RMSE, and the LIDAR and SRTM 30-m DEMs have the largest errors. The two NED DEMs, which do not differ much in accuracy, have the moderate level of RMSE.

2.3. Field observations

Water discharge and total suspended solid values for watersheds 5 and 6 were measured at the monitoring sites on Paradise Creek every two weeks starting March 1999. For Watershed 5, the observation lasted till December 1999 with 18 records; for Watershed 6, the observation lasted till June 2002 with 65 records. Daily values of runoff and sediment yield were calculated from these records using linear interpolation method. Annual values were determined through integration, and their averages were calculated. For Watershed 5, the average annual runoff is 138,940m³ and the sediment yield is 1.38t. For Watershed 6, the average annual runoff is 406,500m³ and the sediment yield is 4.55t.

2.4. WEPP application to Watershed 5

In this study, WEPP was first applied to Watershed 5, the smaller of the two watersheds. Four input files that describe the climate, management, soils, and topography were prepared. Since the study area is relatively small with homogeneous conditions, the

climate, management, and soil input for each hillslope and channel were assumed to be the same.

Existing climate data for the study area, including daily maximum temperature, minimum temperature, and precipitation, were downloaded from the National Climatic Data Center (NCDC) Local Weather Observation Station Record website. The data were observed in City of Moscow University of Idaho station, the closest weather station to the study area. WEPP climate input requires additional parameters such as tp, ip, solar radiation, dew point temperature, etc. Cligen Weather Generator was therefore used to generate the remaining parameters while reserving the observed temperature and precipitation data. A total of 30 years of climate input were prepared for the period of 1973 to 2002.

The management input was generated using the default file built in the WEPP model for a 20-year-old forest with 100 percent ground cover, which corresponds to the forest condition in the study area.

The soil input was based on the default file built in the WEPP model for a 20-year-old forest with silt loam texture. In addition to the adjustment made to the input parameters to meet the requirements of the WEPP v2005 model, several key parameters were adjusted in order to achieve satisfactory agreement between the WEPP predicted and the field observed runoff and sediment yield values. The bedrock hydraulic conductivity was set to $3.6e-6$ mm/h based on the physical characteristics of granite (Domennico and Schwartz 1998) underneath the study area. The anisotropy ratio of the soil was set to 50. The surface soil hydraulic conductivity was set to 140mm/h. The rock contents in the soil input were increased from 20% to 40% for hillslopes, and to 50% for channels. The default soil depth of 400mm, which is believed to be the depth where the impervious soil layer begins, was adopted for the study

area because it reasonably represents the depth to which most hydrologic functions occur in the soil.

The topographic input, including both hillslope profiles and watershed channel files, were derived from each of the six prepared DEMs through the TOPAZ application in GeoWEPP. In TOPAZ, the Critical Source Area (CSA) was set to 10ha and the Minimum Source Channel Length (MSCL) to 100m to make the derived channel networks and watershed structures as close to USGS DRG (digital raster graphic) maps as possible.

Several parameters in the GeoWEPP generated channel structure file were adjusted. The channel erodibility factor was decreased from 0.0006 to 0.0005 s/m. The channel critical shear stress was increased from 100 to 120 N/m². These adjustments represented more stable channels and larger-sized rocks in the channels. The default values in the channel file for depth to nonerodible layer in mid-channel and along the side of the channel were decreased from 0.5 to 0.04m and from 0.1 to 0.03m, respectively, to better represent the streams in the study area.

The above parameter calibration was not carried out in favor of any DEMs, but was for all the six DEMs as a group. During the calibration iterations, the six DEMs responded in the same trend of increasing or decreasing erosion prediction to each of the adjusted parameters.

Because of the differences in DEM resolution and accuracy, the derived watersheds have slightly different areas (Table 10 and 11). The numbers of hillslopes and channels also varied in Tables 10 and 11.

The WEPP model was then executed for Watershed 5 using the adjusted inputs. Six runs in total were made using six topographic input files generated from the six DEMs. The

other inputs of climate, soil, and management, were kept the same for the runs in order to test the effects of only the DEMs on the model predictions.

2.5. WEPP application to Watershed 6

The WEPP model was subsequently applied to Watershed 6, which covers a larger area and has a longer period of runoff and sediment observation record. To better assess the suitability of the model, all inputs for Watershed 6 were generated using the same methods as for Watershed 5. Parameters calibrated for Watershed 5 were used for Watershed 6 without further adjustment.

3. Results

3.1. Results for Watershed 5

The predicted average annual runoff and sediment yield for the two watersheds were obtained from the yearly values simulated by WEPP for the 30-year period. The predicted values were then compared with the observed data. Compared to the observed data, all predictions overestimated both runoff and sediment yield in Watershed 5 (Table 10). But the differences among the runoff predictions (63% to 74% greater than the observed value) were much less than the sediment yield predictions (52.2% to 921.7% higher than the observed value). All three 30-m DEMs led to overestimations of sediment yields by more than 100% of the observed value. Among them, the SRTM DEM had the poorest result, followed by the LIDAR DEM and the NED DEM. The finer-resolution DEMs improved the model performance greatly. The LIDAR 10-m and 4-m DEMs and the NED 10-m DEM generated smaller overestimations of sediment yield, all under 100% off the observed value. The

LIDAR 10-m DEM provided the closest predictions of runoff and sediment yield, followed by the LIDAR 4-m and NED 10-m DEMs.

Table 10. The GeoWEPP derived watershed areas, number of hillslopes, number of channels, and the WEPP predicted average annual runoff and sediment yield using different DEMs for Watershed 5.^a

DEM	Area (ha)	Number of Hillslopes	Number of Channels	Runoff (m ³ /year)	Sediment Yield (t/year)
LIDAR 30-m	112.94	13	5	241118 (73.5) ^b	5.6 (305.8) ^b
NED 30-m	110.72	13	5	238844 (71.9)	4.0 (189.9)
SRTM 30-m	112.31	18	7	235007 (69.1)	14.1 (921.7)
LIDAR 10-m	106.06	13	5	226973 (63.4)	2.1 (52.2)
NED 10-m	111.66	18	7	232654 (67.5)	2.5 (81.2)
LIDAR 4-m	107.26	13	5	229098 (64.9)	2.2 (59.4)

a. GeoWEPP uses TOPAZ to derive the topographic parameters. As a comparison, the same parameters derived from ArcGIS 9® using LIDAR 4-m are: 106.43ha for the watershed area, 11 for the number of hillslopes, and 6 for the number of channels.

b. shown in parentheses are errors in percentage.

3.2. Results for Watershed 6

Results for Watershed 6 (Table 11) showed a different pattern of model predictions compared to those for Watershed 5. All six DEMs had underestimated runoff values. But only four of them had overestimated sediment yields. The predictions were much closer to the observed data than those for Watershed 5. The SRTM DEM still had the poorest predictions among the six DEMs for both runoff and sediment yield. Predictions from the other five DEMs were all less than 10% from the observed runoff and less than 40% from the observed sediment yield. Among the 30-m DEMs, the NED DEM and the LIDAR DEM provided very close predictions with the LIDAR DEM slightly better than the NED DEM in predicting runoff. The finer DEMs, LIDAR 10-m and 4-m and NED 10-m DEMs, did not improve the model performance as much as for Watershed 5. Still, they generated better

predictions than the 30-m DEMs; the only exception was the NED 10-m DEM, which actually performed slightly worse than the NED 30-m DEM for the runoff prediction. The LIDAR 10-m DEM generated a very good prediction in runoff and the closest prediction in sediment yield. The LIDAR 4-m DEM had the closest prediction in runoff and the second best prediction in sediment yield. Both LIDAR DEMs distinguished themselves from other DEMs by having very close predictions and consistent underestimation patterns for runoff and sediment yield. Overall, LIDAR 10-m DEM performed the best in predicting runoff and sediment yield for both Watershed 5 and 6.

Table 11. The GeoWEPP derived watershed areas, number of hillslopes, number of channels, and the WEPP predicted average annual runoff and sediment yield using different DEMs for Watershed 6.^a

DEM	Area (ha)	Number of Hillslopes	Number of Channels	Runoff (m ³ /year)	Sediment Yield (t/year)
LIDAR 30-m	178.27	22	9	375795 (-7.6) ^b	6.2 (36.3) ^b
NED 30-m	176.14	27	11	374452 (-7.9)	6.2 (36.3)
SRTM 30-m	175.96	27	11	362753 (-10.8)	9.6 (111.0)
LIDAR 10-m	176.56	28	11	378949 (-6.8)	4.3 (-5.5)
NED 10-m	179.62	28	11	371966 (-8.5)	6.2 (36.3)
LIDAR 4-m	176.83	28	11	383005 (-5.8)	3.9 (-14.3)

a. GeoWEPP uses TOPAZ to derive the topographic parameters. As a comparison, the same parameters derived from ArcGIS 9® using LIDAR 4-m are: 176.60ha for the watershed area, 22 for the number of hillslopes, and 12 for the number of channels.

b. shown in parentheses are errors in percentage.

3.3. Statistical analysis

An analysis of variance (ANOVA) was carried out to test the differences between the model predictions and the observed values. The three dependent variables were the watershed area, runoff, and sediment yield. A significant level (α) of 0.05 was used to

determine whether the differences in the dependent variable as indicated by the calculated F values, were significant.

The results showed that the differences among the watershed areas, as delineated by GeoWEPP and ArcGIS 9®, were not significant (F-value of 1.81, p-value of 0.2435). The observed runoff value and the model predicted runoff values from different DEMs did not differ significantly (F = 0.25, p = 0.9402). However, the observed sediment yield and the model predictions from different DEMs were significantly different (F = 5.23, p = 0.0320).

3.4. Long-term prediction

Long-term (for the period of 1973-2002) runoff and sediment yields predicted by WEPP using the DEM that generated the closest predictions to field observation, which was the LIDAR 10-m DEM, are shown in Figures 7–13. Shown also are the yearly precipitation (Figure 7, 8, 10, 11) and the annual average rainfall intensity (Figure 12, 13).

For both Watershed 5 and 6, the model predicted rather evenly distributed runoff events during the 30-yr period. Most of the runoff events were predicted to occur in late winter and springtime, and were consistent with field observations. Generally, the magnitude of runoff events was related to yearly precipitation and annual average rainfall intensity. The yearly runoff patterns were similar for the 30-yr period except for year 4 and 21, with no or few runoff events occurring.

The sediment yield patterns differed. For both watersheds, the events did not occur evenly in either frequency or magnitude, especially for Watershed 5. Notice that in Figure 8, 9, and 11, the Y-axis of sediment yield is in common log scale, which helps make the minor events visible. For both watersheds, the model predicted a series of large sediment yield

events during the first winter to spring period. The magnitudes of these events were about 1,000 times to the other events. This pattern did not completely correspond to precipitation or rainfall intensity. For Watershed 5, the sediment yield events mainly occurred during the first five years and the last six years. In between, there was only one average-sized event in year 17. Figure 9 is a detail of the first 16 months shown in Figure 8. It shows the high frequency and high magnitude events occurring at the beginning of the simulation. This is correspondent with the algorithm used in WEPP to simulate channel erosion. WEPP simulates soil detachment to occur initially from the channel bottom until the nonerodible layer is reached. Once the channel reaches the nonerodible layer, it begins to widen and the erosion rate decreases until the flow is too shallow to cause detachment (Ascough II et al. 1995). In this case, the concentrated simulation of sediment yield during the first winter to spring period represents the initial detachment occurring before the nonerodible layer is reached. The frequency of sediment yield events in Watershed 6 was much more even compared to that of Watershed 5. Events were predicted for almost every year except for the winters of year 4, 12, 27, and 28, which corresponded to the low precipitation for those years.

4. Discussion

The study has found that LIDAR DEMs are potentially very useful tools for erosion modeling. The LIDAR 4-m and 10-m DEMs had the highest accuracy and generated the best sediment yield predictions. Overall, the performance of LIDAR 10-m DEM was better than LIDAR 4-m DEM. This finding suggests that a 10-m resolution may be adequate to derive watershed topographic and hydrologic parameters assuming that the accuracy of the DEM is high. This finding is consistent with Zhang and Montgomery's (1994) claim that 10-m is the

proper resolution and the rational compromise between increasing resolution and data volume for simulating geomorphic and hydrological processes. The LIDAR 30-m DEM reveals another aspect of LIDAR data important for soil erosion modeling. It did not show any superiority to the NED 30-m DEM in terms of the accuracy or the sediment yield predictions. This suggests that large grid spacing in a LIDAR-extracted DEM can result in loss of data and high errors (Smith et al. 2003). In other words, a 30-m resolution may be too coarse to generate high-accuracy DEMs from very accurate raw LIDAR points.

The SRTM 30-m DEM may not be a good source for predicting sediment yields. Besides its coarse resolution, its elevations are canopy based and are not appropriate for predicting erosion in small forested watersheds. The NED 10-m DEM was slightly more accurate than the NED 30-m DEM in this study. For sediment yield predictions, however, they did not differ substantially, thus suggesting they are of the same quality for erosion modeling.

Soil erosion predictions were better for the larger watershed than for the smaller watershed. Although the WEPP input parameters were calibrated for the smaller watershed, the model predictions for the larger watershed were actually closer to the observed data than for the smaller watershed. The variation of the sediment yield predictions for the larger watershed was less than that for the smaller watershed. For instance, the sediment yield predictions from the LIDAR 30-m, NED 30-m, and NED10-m DEMs were identical for the larger watershed, but varied greatly for the smaller watershed. Topographically, the smaller watershed had steeper slopes and more complex terrain, which made the topographic input more important in the simulation. Since many forests are found in mountainous areas with large slope variations and complex terrain, carefully selecting the appropriate DEM with

proper accuracy and resolution is therefore critical to simulate hydrologic and erosion processes in forested areas.

Previous studies in WEPP applications have shown unsatisfactory simulations of forest watershed hydrology and erosion. Elliot et al. (1996) found that WEPP predicted only 50% of the observed runoff and 10 times more sediment yield than was observed in a harvested forest watershed. Koopman (2002) claimed that using 30m DEMs, GeoWEPP over-predicted runoff by 10-50 times and under-predicted sediment yield by 50% than the observed values in small forest watersheds. Compared to these previous studies, this study has shown that WEPP v2005 can generate satisfactory predictions of runoff and sediment yield for forest watersheds by using the proper DEMs. The best predictions of runoff and sediment yield in this study were both under 6% off the observed values.

5. Summary and conclusions

This research project studied the effects of DEM resolution and accuracy on watershed hydrology and water erosion prediction at watershed scale by applying WEPP v2005 under forest setting. Six DEMs were prepared for two small forest watersheds located on Moscow Mountain in northern Idaho. They were the LIDAR 30-m, 10-m, and 4-m DEMs, the NED 30-m, and 10-m DEMs, and the SRTM 30-m DEM. These DEMs were used to calculate topographic and hydrologic parameters that served as inputs in WEPP. The model predictions were then compared with the runoff and sediment yield data observed at the watershed outlets. Long-term runoff and sediment yield predictions were also examined.

This study has found that DEMs with different resolutions and accuracy may lead to significantly different sediment yield predictions in WEPP. In general, as DEM resolution

became finer, its accuracy was higher; the resulting sediment yield estimates approached to the observed values. Conversely, as DEM resolution became coarser, its accuracy was lower; the resulting sediment yield estimates departed from the observed values. The 10-m DEMs led to better sediment yield predictions than the 30-m DEMs. When holding the resolution constant, in general, DEMs with high accuracy predicted better in sediment yields than DEMs with low accuracy. The LIDAR 10-m DEM performed better than the NED 10-m DEM, because the LIDAR DEM was more accurate than the NED DEM (Table 7).

The other finding is that, generally, the WEPP simulations using fine-resolution DEMs did not predict runoff significantly better than simulations using coarser-resolution DEMs for long-term average values. DEMs with the same resolution but from different sources did not result in significantly different runoff simulations, either. The importance of this finding lies in its implication that fine-resolution DEMs may not be necessary to estimate runoff at watershed scale. Instead of the costly, fine-resolution LIDAR DEMs, the most widely used, publicly accessible DEMs, such as NED DEMs at 10-m and 30-m resolutions, are appropriate for the model.

The study has also found that WEPP v2005 can generate satisfactory predictions of runoff and sediment yield for forest watersheds by using proper DEMs. High resolution and accuracy DEMs, such as the LIDAR 10m DEM can be used in WEPP to simulate long-term runoff and sediment yield patterns. The model tends to predict substantially high sediment yields for the first two-year period, which is not completely consistent with the precipitation and rainfall intensity pattern. Further effort is therefore needed to improve the channel erosion algorithm in WEPP. The model simulated runoff and sediment yield patterns can be used to improve the understanding of water erosion in forested watersheds.

6. Acknowledgement

The authors thank Dr. William Elliot (Rocky Mountain Research Station, USDA Forest Service) for his critical guidance and great suggestions in model simulation. Dr. Erin Brooks (Department of Biological and Agricultural Engineering, University of Idaho) and Bill Dansart (Idaho Soil Conservation Commission) provided the raw field data of runoff and sediment yield. Sue Miller, Dr. Andy Hudak and Jeff Evans (Rocky Mountain Research Station, USDA Forest Service) helped in GPS application and LIDAR data processing. Their time and efforts are very much appreciated.

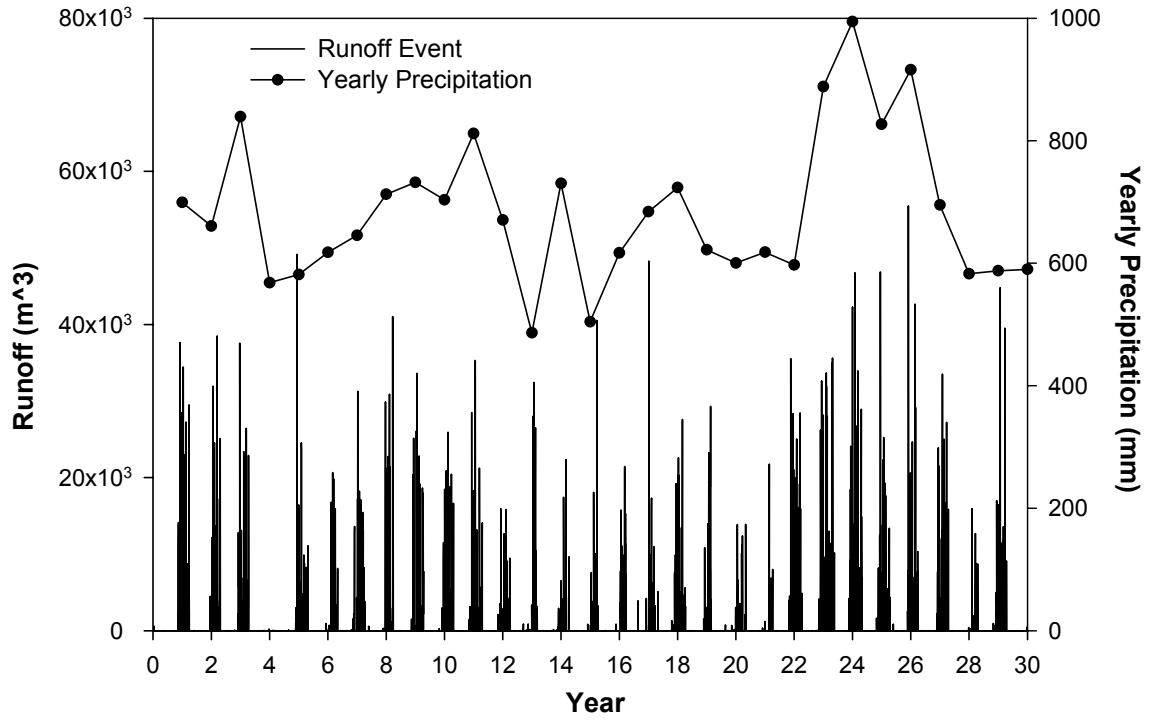


Figure 7. Yearly precipitation vs. 30-yr simulation of runoff events based on LIDAR 10-m DEM for Watershed 5

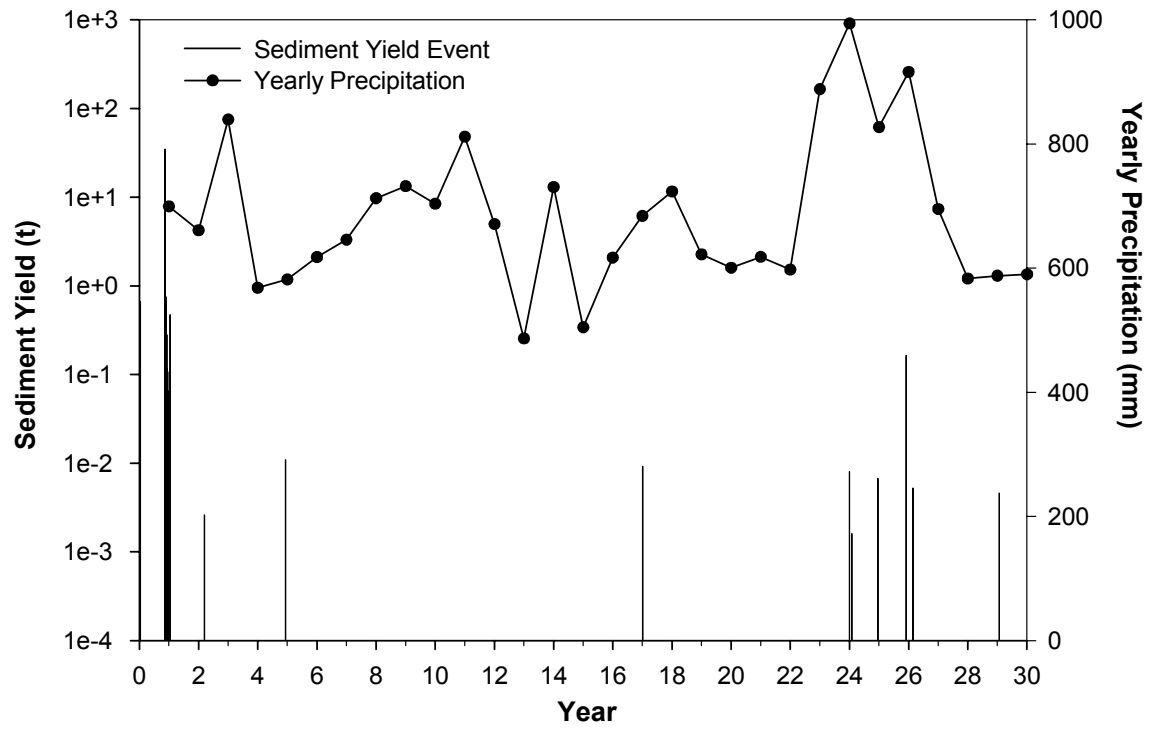


Figure 8. Yearly precipitation vs. 30-yr simulation of sediment yield events based on LIDAR 10-m DEM for Watershed 5. Note Y-axis is in log scale.

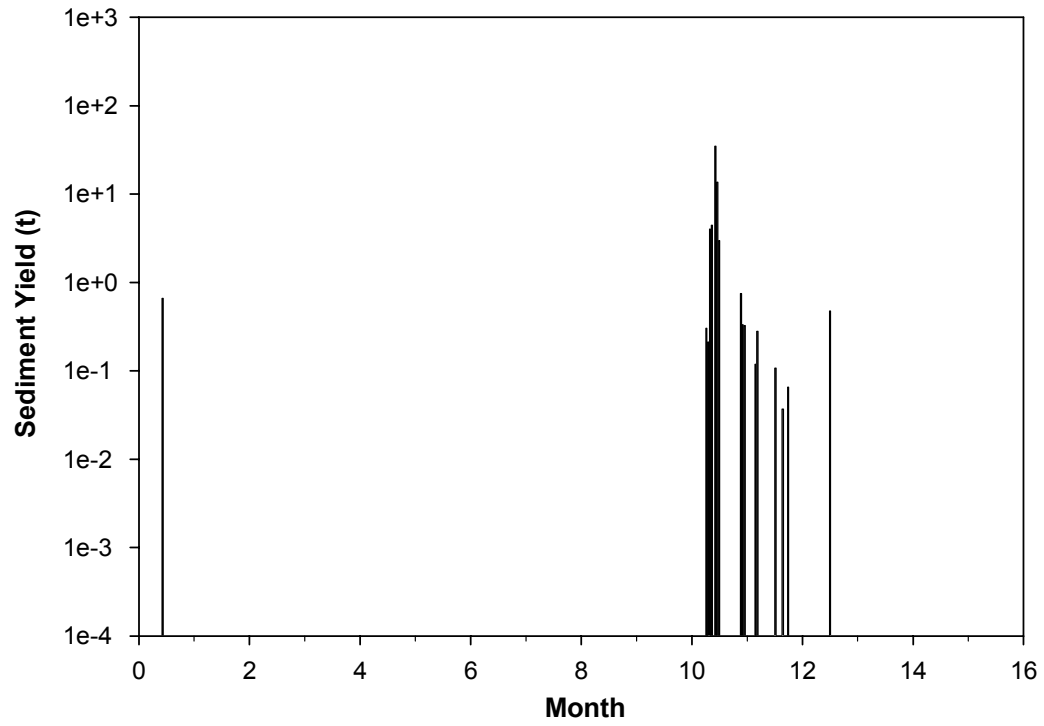


Figure 9. The first 16 months of the 30-yr simulation of sediment yield events based on LIDAR 10-m DEM for Watershed 5. Note *Y*-axis is in log scale.

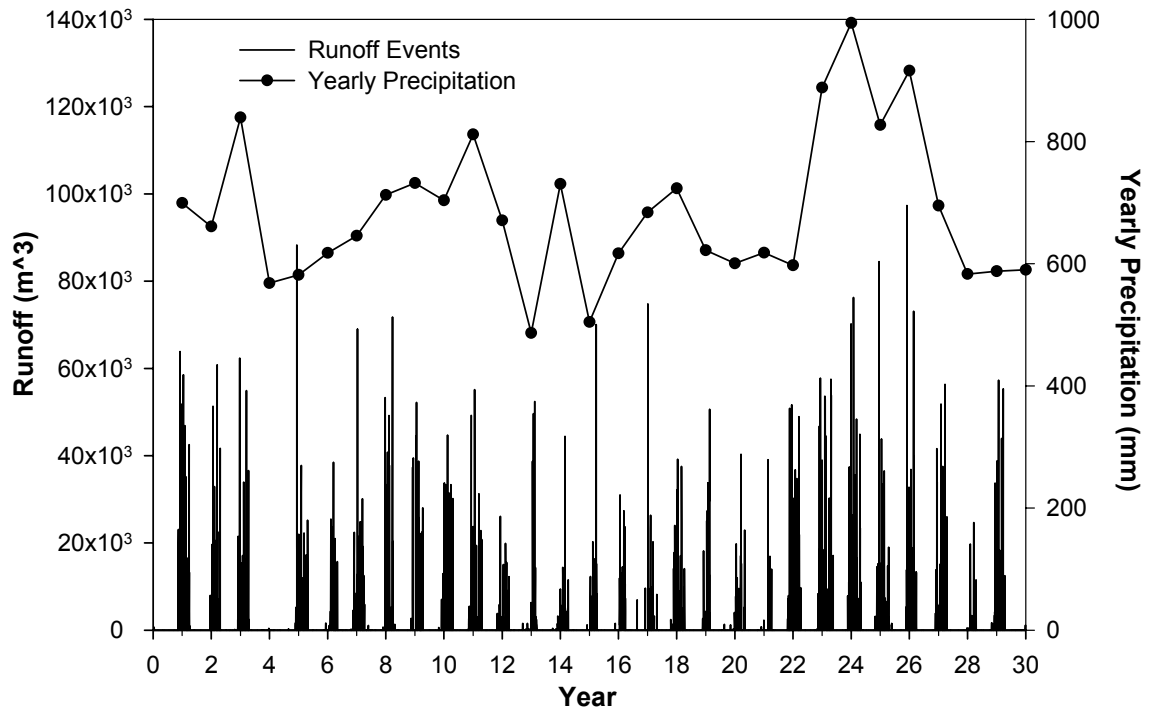


Figure 10. Yearly precipitation vs. 30-yr simulation of runoff events based on LIDAR 10-m DEM for Watershed 6.

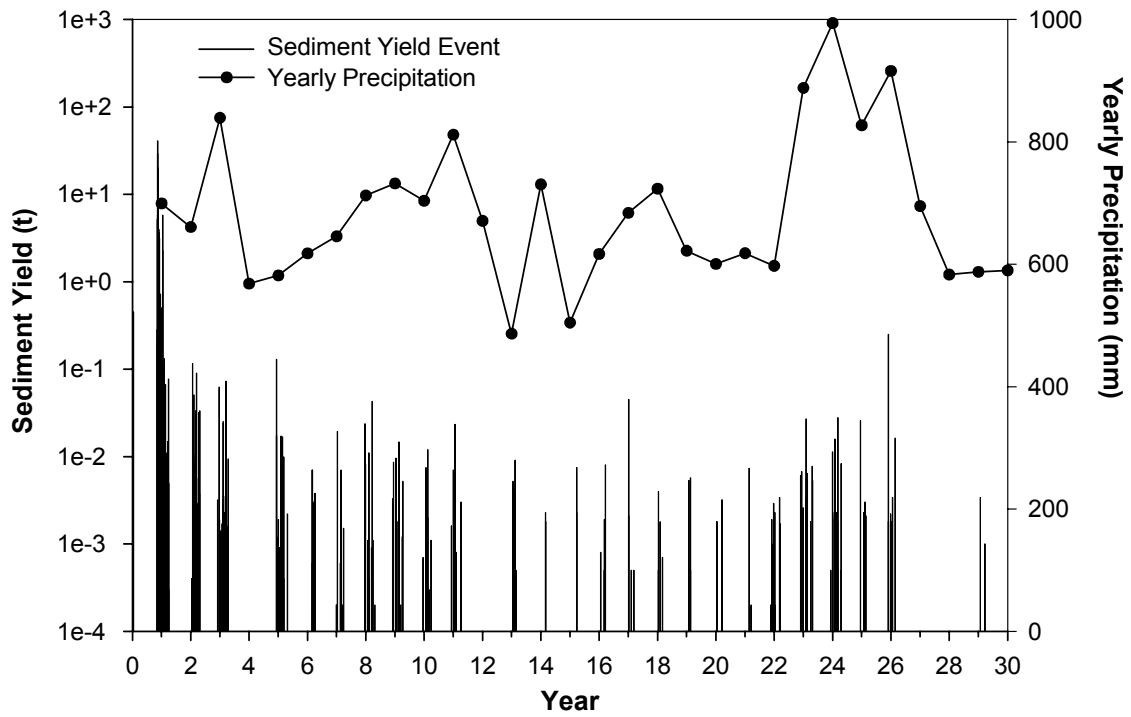


Figure 11. Yearly precipitation vs. 30-yr simulation of sediment yield events based on LIDAR 10-m DEM for Watershed 6. Note Y-axis is in log scale.

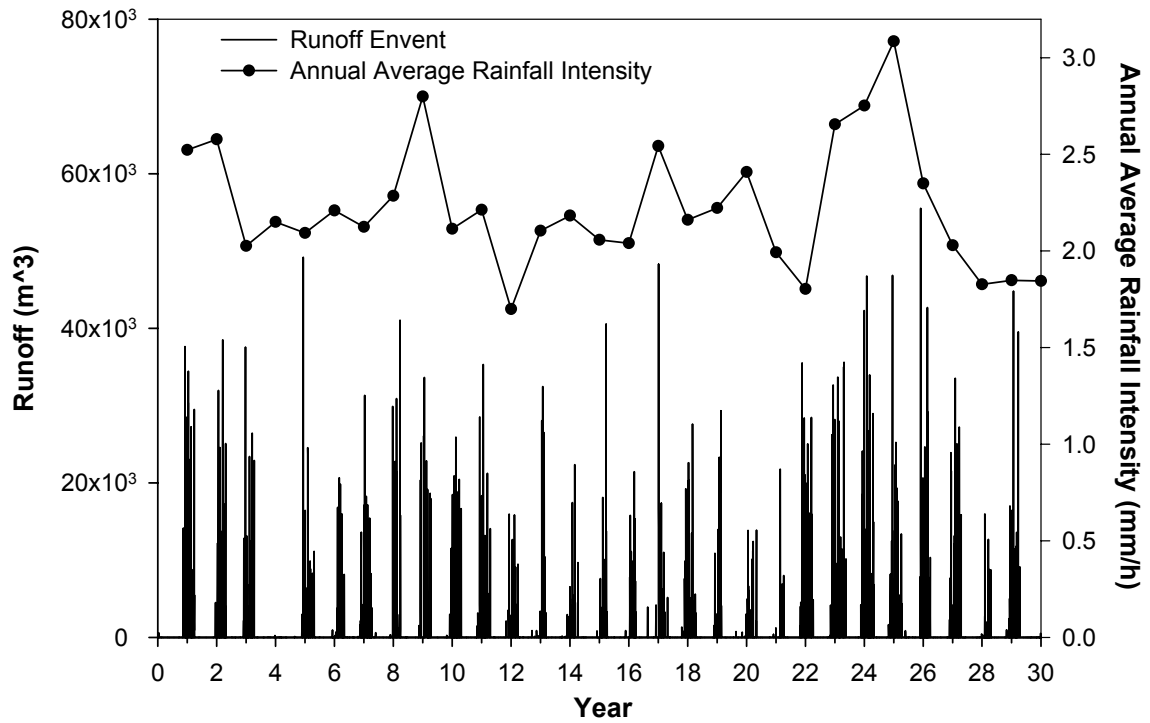


Figure 12. Annual average rainfall intensity vs. 30-yr simulation of runoff events based on LIDAR 10-m DEM for Watershed 5. The annual average rainfall intensity is the average of the intensity of each rainfall event in a year.

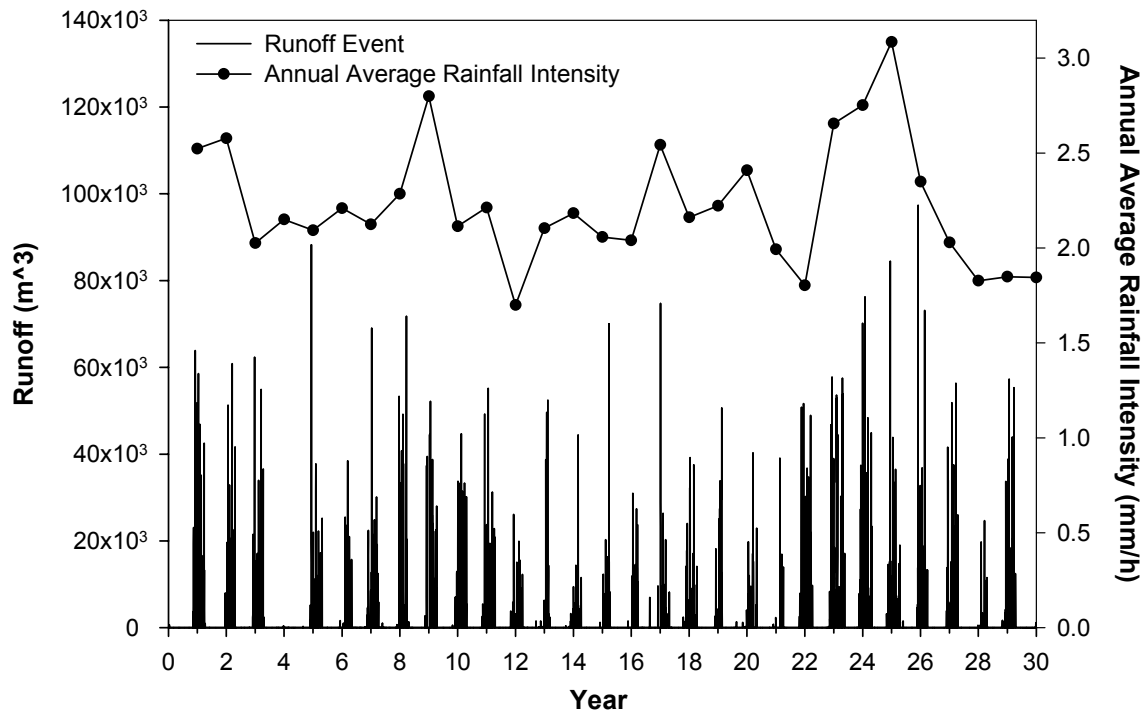


Figure 13. Annual average rainfall intensity vs. 30-yr simulation of runoff events based on LIDAR 10-m DEM for Watershed 6. The annual average rainfall intensity is the average of the intensity of each rainfall event in a year.

7. References

- Ascough II, J.C., Baffaut, C., Nearing, M.A., Flanagan, D.C., 1995, Watershed model channel hydrology and erosion processes. In *USDA Water Erosion Prediction Project: Hillslope Profile and Watershed Model Documentation*, Flanagan DC, Nearing MA (eds). Ch. 13. NSERL Rep., 10. USDA-ARS National Soil Erosion Research Laboratory, West Lafayette. IN.
- Chang, K.T., and Tsai, B.W., 1991, The effect of DEM resolution on slope and aspect mapping. *Cartography and Geographic Information Systems*, **18**(1), pp. 69-77.
- Cochrane, T.A., 1999, Methodologies for watershed modeling with GIS and DEMs for the parameterization of the WEPP model. Ph.D. thesis, Purdue University.
- Desmet, P.J.J., and Govers, G, 1996, A GIS-procedure for automatically calculating the USLE LS factor on topographically complex landscape units. *Journal of Soil and Water Conservation*, **51**(5), pp. 427-433.
- Domennico, P.A., and Schwartz, F.W., 1998, *Physical and Chemical Hydrogeology* (second edition). John Wiley & Sons, Inc.
- Elliot, W.J., Luce, C.H., and Robichaud, P.R., 1996, Predicting sedimentation from timber harvest areas with the WEPP model. In *Proc. Sixth Federal Interagency Sedimentation Conf.*, Las Vegas, NEV, pp. 46-53.
- Flanagan, D.C., and Livingston, S.J., 1995, WEPP user summary, USDA-Water Erosion Prediction Project (WEPP). (W. Lafayette, IN: USDA-ARS National Soil Erosion Research Laboratory).
- Fahsi, A., 1989, The effect of spatial resolution of digital elevation model data on map characteristics. M. S. thesis, University of Idaho.
- Florinsky, I.V., 1998, Accuracy of local topographic variables derived from digital elevation models. *International Journal of Geographical Information Systems*, **12**, pp. 47-61.
- Gao, J., 1998, Impact of sampling intervals on the reliability of topographic variables mapped from grid DEMs at a micro-scale. *International Journal of Geographical Information Systems*, **12**, pp. 875-890.
- Garbrecht, J., and Martz, L.W., 1997, TOPAZ: Topographic Parameterization Software. El Reno, Okla.: USDA Agricultural Research Service, Grazinglands Research Laboratory. Available online at: <http://grl.ars.usda.gov/topaz/TOPAZ1.HTM>. (accessed 22 September 2004).

Gerrard, A.J.W., and Ronbinson, D.A., 1971, Variability in slope measurement: a discussion of the effects of different recording intervals and microrelief in slope studies. *Transactions, Institute of British Geographers*, **54**, pp. 45-54.

Gertner, G., Wang, G., Fang, S., Anderson, A.B., 2002, Effect and uncertainty of digital elevation model spatial resolution on predicting the topographical factor for soil loss estimation. *Journal of Soil and Water Conservation* **57**(3), pp.164-174.

Hill, J.M., Graham, L.A., and Henry, R.J., 2000, Wide-area topographic mapping and applications using airborne Light Detection and Ranging (LIDAR) technology. *Photogrammetric Engineering & Remote Sensing*, **66**, pp. 908-914.

Jenson, S.K., and Domingue, J.O., 1988, Extracting topographic structure from digital elevation data for geographic information system analysis. *Photogrammetric Engineering and Remote Sensing*, **54**, pp. 1593-1600.

Jenson, S.K., 1991, Application of hydrologic information automatically extracted from digital elevation models. *Hydrological Processes*, **5**, pp. 31-44.

Koopman, M., 2002, Geo-spatial prediction tools in forest management: Modeling post-burn hydrology of soil erosion in three western forests. MA thesis, Buffalo, State University of New York.

Kraus, K., and Pfeifer, N., 1998, Determination of terrain models in wood areas with airborne laser scanner data. *ISPRS Journal of Photogrammetry and Remote Sensing*, **53**, pp. 193-203.

Lee, H.S., and Younan, N.H., 2003, DTM extraction of LIDAR returns via adaptive processing. *IEEE Transaction on Geoscience and Remote Sensing*, **41**(9), pp. 2063-2069.

Lo, C.P., and Yeung, A.K.W., 2002, In *Concepts and Techniques of Geographic Information Systems*, (Prentice Hall Inc).

Luce, C.H., 1995, Forests and wetlands; 267-274. In *Environmental Hydrology*, Ward AD, Elliot WJ (eds). CRC Lewis Publishers, pp. 253-284.

Mitasova, H., Hofierka, J., Zlocha, M., Iverson, L.R., 1996, Modeling topographic potential for erosion and deposition using GIS. *International Journal of Geographical Information Systems* **10**(5), pp. 629-641.

Renschler, C.S., and Harbor, J., 2002, Soil erosion assessment tools from point to regional scales – the role of geomorphologists in land management research and implementation. *Geomorphology*, **47**, pp.189-209.

Renschler, C.S., 2003, Designing geo-spatial interfaces to scale process models: the GeoWEPP approach. *Hydrological Processes*, **17**, pp. 1005-1017.

Smith, S.L., Holland, D.A., and Longley, P.A., 2003, The effect of changing grid size in the creation of laser scanner digital surface models. *Proceedings of the 7th International Conference on GeoComputation*, 8 - 10 September 2003, University of Southampton, United Kingdom

The Idaho Division of Environmental Quality, Lewiston Regional Office. 1997. Paradise Creek TMDL – water body assessment and total maximum daily load.

Turner, A.K., 2000, LIDAR provides better DEM data. *GEOWorld*, **13**(11), pp. 30-31.

Vosselman, G., 2000, Slope based filtering of laser altimetry data. *International Archive of Photogrammetry and Remote Sensing B4*, **33**, pp. 958–964.

Wu, J.Q., Xu, A.C., Elliot, and W.J., 2000, Adapting WEPP for forest watershed erosion modeling. *Paper No. 002069. The 2000 International ASAE Meeting*, 9-12 July, Milwaukee, WI. St. Joseph, MI.

Zhang, K., Chen, S.C., Whitman, D., Shyu, M.L., Yan, J., and Zhang, C., 2003, A progressive morphological filter for removing nonground measurement from airborne LIDAR data. *IEEE Transaction on Geoscience and Remote Sensing*, **41**(4), pp. 872-882.

Zhang, W.H., and Montgomery, D.R., 1994, Digital elevation model grid size, landscape representation, and hydrologic simulations. *Water Resources Research* **30**(4), pp. 1019-1028.

Chapter 4

General conclusions and recommendations for further research

1. General conclusions

This study has found that DEMs with different resolutions and sources can generate varied watershed shapes and structures and extract different hillslope and channel systems, which can in turn result in significantly different sediment yield predictions in the WEPP model. In general, as DEM resolution became finer, its accuracy was higher, the landscape was more precisely and accurately represented, and the sediment yield estimates approached closer to the observed values. Conversely, as DEM resolution became coarser, its accuracy was lower, and the sediment yield estimates departed from the observed values. This study has also found that high resolution and accuracy DEMs can be used in the WEPP model to simulate long-term runoff and sediment yield patterns.

Based on the results of the study, hypothesis 1 on the effect of DEM resolution is partially confirmed. Finer-resolution DEMs generated better presentations of watershed shape and structure. The 10-m DEMs generated much closer sediment yield predictions to the observed data than the 30-m DEMs. However, finer-resolution DEMs did not lead to significantly better runoff predictions than coarser-resolution DEMs. Statistically, all six DEMs (LIDAR 30-m, 10-m, 4-m, NED 30-m, 10-m, and SRTM 30-m DEMs) performed the same in runoff prediction. Moreover, the 4-m DEM did not generate closer sediment yield predictions to the observed data than the 10-m DEM. Therefore, this study suggests that a 10-m DEM can be used for deriving topographic and hydrologic parameters and for predicting sediment yield in small watersheds, assuming that the DEM's accuracy is sufficiently high.

Hypothesis 2 is partially confirmed. This study confirms that when holding the resolution constant, DEM sources (LIDAR, NED, SRTM) with higher accuracy generated better presentations of watershed shape and structure and closer predictions of sediment yield

to the observed data. The hypothesis is also partially rejected because DEMs with the same resolution but from different sources did not produce significantly different runoff simulations. Statistically, all six DEMs performed the same in runoff prediction. Moreover, the SRTM 30-m DEM, which had a higher accuracy than the LIDAR 30-m DEM, led to the poorest prediction of sediment yield. The SRTM 30-m DEM may not be a good data source for generating topographic and hydrologic attributes in forested areas or for predicting sediment yields based on this study.

Hypothesis 3 is the only hypothesis that is fully confirmed. This study proves that, when using the same DEM, the characteristics of the watershed terrain have substantial effects on the WEPP model predictions. In this study, the smaller watershed has a more complex topography and larger slope variations than the larger watershed. Topographic features extracted from the DEMs were less realistic, and the runoff and sediment yield predictions were less accurate, in the smaller watershed than in the larger watershed. It is therefore critical to select the appropriate DEM with proper accuracy and resolution for simulating hydrologic and erosion processes in mountainous areas with large slope variations.

2. Recommendations for further research

This study has discussed the effects of DEM resolution and source on deriving topographic and hydrologic parameters. The third factor affecting the accuracy of these derived parameters is the DEM processing algorithm used for routing flow and computing contributing areas (Garbrecht and Martz, 2000). A variety of algorithms are currently available. The most commonly used is the D8 flow routing algorithm that allows flow to one

of only eight neighbors based on the direction of steepest descent. The TOPAZ in GeoWEPP is based on the D8 method. One major weakness of the D8 algorithm is that although the center cell can receive upstream flow from several sources, the downstream flow can only be in one direction, either cardinal or diagonal. Such an algorithm is not suitable for areas where divergent flows occur, e.g., along convex slopes and ridges (Costa-Cabral and Burges 1994, Wilson and Gallant 2000). This algorithm is also criticized because it tends to predict unrealistic flow in parallel lines along preferred directions (Moore et al. 1993).

An alternative to the D8 algorithm is the Dinf method developed by Tarboton (1997). The Dinf procedure represents flow direction as a single angle taken as the steepest downward slope on the eight triangular facets centered at each grid point. Upslope area is then calculated by proportioning flow between two downslope pixels according to how close this flow direction is to the direct angle to the downslope pixel. This procedure offers improvements over the D8 procedure by not restricting flow to only one of eight possible directions (Figure 14).

Further effort may be devoted to applying the Dinf algorithm to extract topographic and hydrologic parameters and to use them as inputs in WEPP to simulate runoff and sediment yield. Research on the effect of the flow routing algorithm would extend the scope and deepen our understanding of the relationship between DEMs, topographic and hydrologic parameters, and soil erosion simulations.

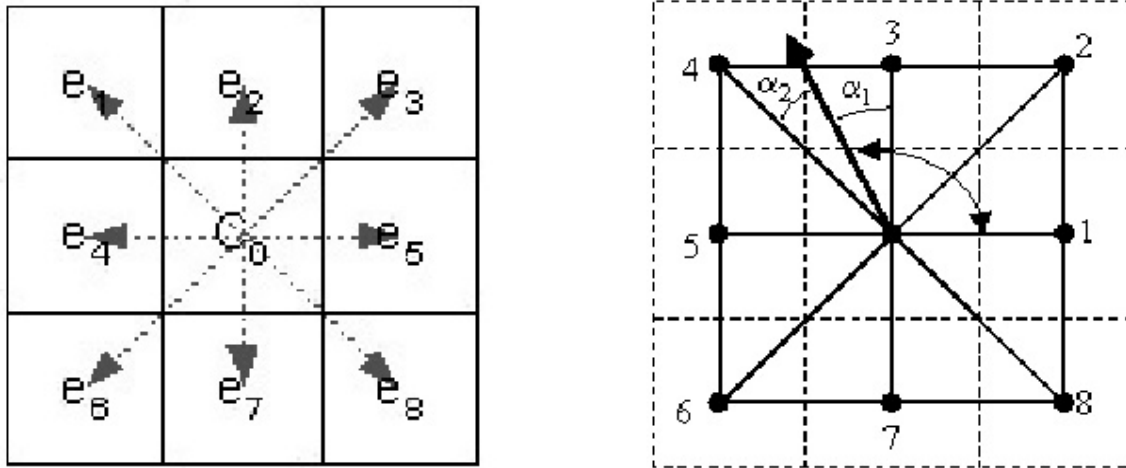


Figure 14. The D8 flow routing algorithm vs. the Dinf method.

3. References

Costa-Cabral, M.C., and Burges, S.J., 1994, Digital elevation model networks (DEMON): a model of flow over hillslopes for computation of contributing and dispersal areas. *Water Resources Research*, **30**, pp. 1681-1692.

Garbrecht, J., and Martz, L.W., 2000, Digital elevation model issues in water resources modeling. In *Hydrologic and Hydraulic Modeling Support with Geographic Information Systems*. D. Maidment, and D. Djokic (Ed.), (Redland, CA: ESRI Press).

Moore, I.D., Turner A.K., Wilson, J.P., Jenson, S.K., and Band, L.E., 1993, GIS and land-surface-subsurface process modelling. In *Environmental Modeling with GIS*, M.F. Goodchild, B.O. Park, and L.T. Styart (Ed.), pp. 213–230 (Oxford, UK: Oxford University Press).

Tarboton, D.G., 1997, A new method for the determination of flow directions and upslope areas in grid digital elevation models. *Water Resources Research* **33**(2), pp. 309-319.

Wilson, J.P., and Gallant, J.C., 2000, *Terrain Analysis: Principles and Applications*. (John Wiley & Sons, Inc).

Appendix A
Literature review

1. Digital elevation model (DEM)

DEMs (digital elevation models) are usually organized into one of the three data structures: regular grids, TIN (triangulated irregular networks), and contours. In this study, the term DEM refers only to the regular square-grid digital elevation model.

1.1. DEM accuracy

Many DEMs contain errors that were generated during the production procedures. The errors contained in the grid-based DEMs are classified as either global or relative (Moore et al. 1991). Global errors are systematic errors in DEMs. One of the most pervasive global errors is the mismatching elevation along the boundaries of adjacent 7.5-minute DEMs. DEMs may also contain noticeable horizontal striping, which results from systematic sampling errors when creating the DEM (Garbrecht and Martz 2000). This is most noticeable on integer data in flat areas. Global errors can usually be corrected by applying transformations including linear or nonlinear translation, rotation, and scaling to the whole DEM.

Relative errors in DEMs occur when a few elevations have obvious errors relative to the neighboring elevations, usually in the form of either sinks or peaks. A sink, also called a depression or pit, is an area surrounded by higher elevation values. It is an area of internal drainage. Some sinks may be natural, particularly in glacial or karst areas (Mark 1983), although many sinks are imperfections in the DEM. Likewise, a spike or peak is an area surrounded by cells of lower values. These are more commonly natural features, and are less detrimental to the calculation of flow direction. The number of sinks in a given DEM is normally higher for coarser-resolution DEMs. Another common cause of sinks results from

storing the elevation data as an integer number. This can be particularly troublesome in areas of low vertical relief. It is not uncommon to find 1% of the cells in a 30-meter-resolution DEM to be sinks. This can jump sometimes as high as 5% for a 3-arc-second DEM (ArcDoc 2001). Sinks may cause undesirable results when calculating flow direction (Jenson and Domingue 1988). Relative errors, especially sinks, should be removed or filled to ensure proper delineation of basins and streams.

Various algorithms have been developed to produce depressionless DEMs from grid-based DEM (O'Callaghan and Mark 1984, Jenson and Domingue 1988, Hutchinson 1989, 1996). Jenson and Domingue (1988) used the depressionless DEM as a first step in assigning flow directions. Based on a hydrologically realistic algorithm (O'Callaghan and Mark 1984), their procedure removes a depression by increasing its cell value to the lowest cell value surrounding the depression. The procedure is capable of determining flow paths iteratively where there is more than one possible receiving cell and where flow must be routed across flat areas. Hutchinson (1989, 1996) developed the ANUDEM program, which produces grid-based DEMs and calculates values on a regular grid of a discretised smooth surface fitted to large numbers of irregularly spaced elevation data points. The program imposes a global drainage condition that automatically removes spurious sinks where possible, and interpolates the elevation data onto a regular grid by minimizing a suitably weak roughness penalty on the fitted grid values and by simultaneously imposing constraints which ensure connected drainage structure. Hutchinson's algorithm has been incorporated into ARC/INFO command TOPOGRID.

The root mean square error (RMSE) is a commonly used measure to assess the accuracy of a DEM. Based on a sample of control points, the RMSE measures the deviation

between the elevations in a DEM (Z_{est}) and the ‘true’ values of elevation on the terrain (Z_{obs}), where the true values can come from benchmarks, independent field measurements or more accurate data sources. The RMSE is expressed as:

$$\text{RMSE} = \sqrt{\sum_{i=1}^n d_i^2 / n} \quad , \text{ where } d_i = Z_{\text{est}} - Z_{\text{obs}}.$$

DEMs produced by the U.S. Geological Survey (USGS) are classified into three levels of increasing quality. For level 1 DEM, a vertical root mean square error (RMSE) of 7 meters is the targeted accuracy standard, and a RMSE of 15 meters is the maximum permitted. For level 2 DEM, a RMSE of one-half of the original map contour interval is the maximum permitted. And for level 3 DEMs, a RMSE of one-third of the contour interval is the maximum permitted. Most data produced within the last decade fall into the level 2 classification (Garbrecht and Martz 2000).

1.2. NED DEM

The National Elevation Dataset (NED) is a raster product assembled by the USGS. It was originally released by the USGS in June 2000, and has been updated every two months. NED is designed to provide national elevation data in a seamless form with a consistent datum, elevation unit, and projection (USGS <http://seamless.usgs.gov/>). Data corrections were made in the NED assembly process to minimize artifacts, perform edge matching, and fill in sliver areas of missing data. Older DEMs produced by methods that are now obsolete have been filtered during the NED assembly process to minimize artifacts that are commonly found in data produced by these methods. Artifact removal greatly improves the quality of the slope, shaded-relief, and synthetic drainage information that can be derived from the

elevation data. NED processing also includes steps to adjust values where adjacent DEMs do not match well, and to fill in sliver areas of missing data between DEMs. These processing steps ensure that the NED has no void areas and artificial discontinuities have been minimized.

Source data for the NED are selected from the available DEMs according to the following priority ranking: high-resolution elevation data, 10-meter USGS DEMs, 30-meter Level 2 USGS DEMs, 30-meter Level 1 USGS DEMs, 2-arc-second USGS DEMs, and 3-arc-second USGS DEMs. NED data sources have a variety of elevation units, horizontal datums, and map projections. In the NED assembly process the elevation values are converted to decimal meters as a consistent unit of measure, NAD83 is consistently used as horizontal datum, and all data are recast in a geographic projection. In addition to the standard 1-arc-second resolution (approximately 30 meters), NED data for a portion of the United States are available in 1/3-arc-second resolution (approximately 10 meters). These higher-resolution data have been produced where 10-meter DEMs and other high-resolution DEMs are available as NED source data.

1.3. DEM and topographic parameters

DEMs and GIS (geographic information system) have largely replaced traditional methods for extracting topographic parameters for hydrologic applications (Jenson and Domingue 1988, Garbrecht and Martz 2000). There are two main types of topographic parameters that can be automatically extracted from DEMs: the primary topographic parameters, and the secondary or compound parameters (Wilson and Gallant 2000). Primary parameters can be computed directly from DEMs. Secondary parameters involve

combinations of primary attributes and constitute physically based or empirically derived indices that can characterize the spatial variability of specific processes occurring in the landscape (Moore et al. 1991). Primary topographic parameters include (Wilson and Gallant 2000):

Altitude (elevation);

Slope (gradient);

Aspect (slope azimuth);

Plan curvature (contour curvature);

Profile curvature (slope profile curvature);

Flow-path length (maximum distance of water flow to a point in the catchment);

Upslope contributing area (catchment area above a short length of contour);

Specific upslope contributing area (upslope area per unit width of contour);

Catchment area (area draining to catchment outlet);

Dispersal area (area downslope from a short length of contour);

Upslope slope (mean slope of upslope area);

Catchment slope (average slope over the catchment);

Dispersal slope (mean slope of dispersal area);

Upslope length (mean length of flow paths to a point in the catchment);

Catchment length (distance from highest point to outlet);

Dispersal length (distance from a point in the catchment to the outlet);

Upslope height (mean height of upslope area);

Tangential curvature (plan curvature multiplied by slope);

Elevation percentile (proportion of cells in a user-defined circle lower than the center cell).

Most of these topographic parameters are calculated from the directional derivatives of a topographic surface. These derivatives measure the rate at which elevation changes in response to changes in location (x and y). They can be computed directly with a second-order finite difference scheme or by fitting a bivariate interpolation function $z = f(x, y)$ to the DEM and then calculating the derivatives of the function (Moore et al. 1993, Florinsky 1998).

Secondary topographic parameters include (Wilson and Gallant 2000):

- Topographic wetness indices

- Stream-power indices

- Radiation indices

- Temperature indices

These secondary topographic parameters are computed from two or more primary attributes. They are important because they offer an opportunity to describe pattern as a function of process. Those topographic parameters can be utilized to study water redistribution in the landscape and the change of solar radiation received at the surface, which has important hydrological consequences in many landscapes. These parameters may affect soil characteristics, distribution and abundance of soil water, and the susceptibility of landscapes to erosion by water.

1.4. DEM computing algorithm

Besides DEM accuracy and resolution, computing algorithm can also affect primary and secondary topographic parameters derived from DEMs. A variety of algorithms are

available for routing flow and computing contributing areas from DEMs. Among these algorithms, there have been two generic approaches (Zhou and Liu 2002): 1) Single Flow Direction (SFD) algorithms, in which the total amount of flow should be received by a single neighboring cell which has the maximum downhill slope with the current cell; and 2) Multiple Flow Direction (MFD) algorithms, in which the flow from the current cell should be distributed to all lower neighboring cells according to a predetermined rule. D8 and Rho8 algorithms belong to the SFD category, whereas FD8 and FRho8 are examples of the MFD category.

1.4.1. D8 (deterministic eight-node)

The D8 algorithm developed by O'Callaghan and Mark (1984) allows flow to one of only eight neighbors based on the direction of steepest descent. It is the most commonly used method for determining drainage areas and has been incorporated into ArcInfo because of its simple and efficient computation, and strong capability in dealing with local depressions and flat areas (Tarboton 1997).

One major weakness of the D8 algorithm is that, although the center cell can receive upstream flow from several sources, the downstream flow can only be in one direction. This is not suitable for areas where divergent flows occur, such as convex slopes and ridges (Costa-Cabral and Burges 1994, Wilson and Gallant 2000). This popular algorithm is also often criticized because it tends to predict flows in parallel lines along preferred directions that will agree with aspect only if the aspect is a multiple of 45° (Moore et al. 1993). The D8 algorithm is adequate for delineating catchment boundaries. But for calculating the

contribution of contributing area and specific catchment area across hillslopes, the more sophisticated FD8 or DEMON methods are recommended (Wilson and Gallant 2000).

1.4.2. Rho8 (random eight-node)

Developed by Fairfield and Leymarie (1991), Rho8 is a stochastic version of the D8 algorithm in which a degree of randomness is introduced into the flow-direction computation. It simulates more realistic flow networks but still cannot model flow dispersion. Moore et al. (1993) found that Rho8 breaks up the long, linear flow paths produced by the D8 method while generating more single-cell drainage areas.

1.4.3. FD8 & FRho8

They are the modifications of D8 and Rho8 that allow flow divergence to be represented. Both FD8 and FRho8 allow flow to be distributed to multiple nearest-neighbor nodes in upland areas above defined channels and use either the D8 or Rho8 algorithms below points of channel initiation (Moore et al. 1993). FD8 and FRho8 have the advantage of giving more realistic distribution of contributing area in upslope areas, while also eliminating D8's parallel flow paths. But they tend to cause considerable dispersion of flows in valleys, which is considered undesirable because streamlines usually are well defined in valleys.

1.4.4. DEMON (Digital Elevation Model Network Extraction)

DEMON was proposed by Lea (1992) and Costa-Cabral and Burges (1994). It is a completely different approach for modeling flow accumulation and dispersion. It avoids dispersion problems by representing flows in two directions as directed by aspect. Flow is

generated at each pixel (source pixel) and is routed down a stream tube until the edge of the DEM or a pit is encountered. This approach permits the representation of varying flow width over nonplanar topography (similar to contour-based models). The DEMON algorithm was subsequently modified and implemented in the TAPE-G software by Moore and his co-workers (Wilson and Gallant 2000).

1.4.5. Vector-grid method

This method constructs flow lines downhill from each grid cell until they reach a cell with a slope lower than some specified minimum, a boundary line, or some other barrier to calculate upslope contributing areas. These flow lines follow the aspect direction of flow, and they are represented in vector format, avoiding the artificial nature of cell-to-cell flow routing. The points defining the flow lines are computed as the points of intersection of a line constructed in the flow direction given by the aspect angle and a grid cell edge. This algorithm has been implemented as the *r.flow* routine in the GRASS GIS (Mitasova et al.1996)

1.4.6. Dinf (Deterministic infinite-node)

This is a new procedure developed by Tarboton (1997) for representing flow directions and calculating upslope areas. The procedure represents flow direction as a single angle taken as the steepest downward slope on the eight triangular facets centered at each grid point. Upslope area is then calculated by proportioning flow between two downslope pixels according to how close this flow direction is to the direct angle to the downslope pixel. This procedure offers improvements over prior procedures that have restricted flow to eight

possible directions (introducing grid bias) or proportioned flow according to slope (introducing unrealistic dispersion), and is more robust than prior procedures by fitting local planes while retaining a simple grid-based structure.

1.4.7. Summary.

Detailed assessments and comparisons of the performance of many of the existing algorithms have been carried out (Endreny and Wood 2003, Zhou and Liu 2002, Wilson and Gallant 2000). These comparisons showed that the single-flow direction algorithms (D8, Rho8) and the multiple-flow direction algorithms (FD8, FRho8, DEMON, and Dinf) perform differently in most types of landscapes, with the DEMON and Dinf algorithms having the overall best performances.

2. Soil water erosion

Soil water erosion refers to the processes of wearing away of particles of soils and rocks on the Earth's surface by water in form of rainfall or snowmelt. Sediment is the mineral or organic material that is displaced by the forces of water and delivered to water bodies.

2.1. Hillslope and channel erosion

The dominant type of erosion besides landslides includes sheet, rill, and gully erosion on hillslopes, and channel erosion in streams (Foster 1982). Erosions occurring on hillslopes are mainly in the form of rain splash, sheetwash, rill, and gully erosion. Rain splash erosion occurs when raindrops impact and displace exposed soil. Sheet erosion is the removal of a

thin, relatively uniform layer of soil particles. Rill erosion occurs when sheet flow cuts small, separate channels as it moves downslope. Gullies are rills greater than certain size that cannot be obliterated by normal tillage. Exposed soil in rills and gullies is especially vulnerable to rain splash erosion. Gully erosion can be dramatic, contributing large sediment loads to streams.

A variety of factors can cause channel erosion. Most stream channel erosion is caused by the action of instream water. Varying with velocity, flowing water exerts fluid stress on the streambed. When applied stress reaches the point that bed particles begin to move, channel erosion results. The capacity of a stream to carry sediment also increases with stream velocity. Because at a given flow, velocity varies within channels longitudinally and in cross section, channel erosion and sedimentation may occur simultaneously. The magnitude of these processes is affected by flow rate: high flows increase channel erosion, and low flows increase sedimentation or deposition.

2.2. Watershed hydrology and erosion in forested areas

A watershed is an area from which water drains into a particular body of water due to its natural drainage pattern. Hydrologically, a watershed may be conceptualized as having overland flow, stream flow, and subsurface flow components. Erosion and sedimentation occur mainly with overland flow and in channel areas (Foster 1982).

The hydrologic and erosion processes in forests differ from croplands and rangelands. Besides the presence of large amounts of vegetation, steep slopes, and shallow, young, and coarse-grained soils typify forests. Forest soils are often highly conductive and, consequently, subsurface flow is the primary form of water movement instead of surface

runoff (Luce 1995). As a matter of fact, surface runoff is rare on undisturbed forest hillslopes.

Streamflow is the primary medium through which water, sediment, nutrients, and organic material move. In forested areas, streamflow is largely produced by ground water seepage. This is because a portion of water that infiltrates the soil, percolates to the water table, and then flows within the water table, is delivered back to surface waters. Excess water, or water which cannot infiltrate the soil, runs off over the surface. Excess water is produced when water is delivered to a watershed surface faster than it can infiltrate the soil or when the soil is already saturated. There is little storage of water flowing over a forest floor, whereas subsurface storage in soil can be substantial. However, overland flow is much more likely than subsurface flow to cause erosion (Reid 1993).

Sedimentation of surface water is the most common nonpoint-source pollution concern related to forest management activities. Many studies have shown that the most important water-quality problem associated with forestry activities is sedimentation. Areas where soil has been disturbed are subject to erosion, resulting in the downslope movement of sediment after it rains. The movement of sediment downhill is related to the steepness of the slope and soil erodibility. Soil erodibility greatly influences the magnitude of soil erosion and transport. Factors that affect soil erodibility include soil texture, percent organic matter, presence of a litter layer, infiltration rate, and bulk density. Sources of sediment include roads and ditches (particularly at stream crossings), bare soil on steep slopes, cut banks, slope failures and debris flows, and streambank erosion and channel scour.

3. Soil erosion models

3.1. RUSLE

A well-known model of soil erosion is the Revised Universal Soil Loss Equation (RUSLE), the updated version of the Universal Soil Loss Equation (USLE) (Wischmeier and Smith 1965, 1978; Renard et al. 1997). RUSLE predicts the average soil loss carried by runoff from specific field slopes in specified cropping and management systems and from rangeland. RUSLE is a multiplicative model with six factors: $A = R K L S C P$. Where A is the average soil loss, R is the rainfall-runoff erosivity factor, K is the soil erodibility factor, L is the slope length factor, S is the slope steepness factor, C is the crop management factor, and P is the support practice factor (Renard et al. 1997).

Among the six factors in RUSLE, the slope length factor L poses more questions than other factors (Renard et al. 1997). Slope length is defined as the horizontal distance from the point of origin of overland flow to the point where either the slope gradient decreases enough that deposition begins or the flow is concentrated in a defined channel (Wischmeier and Smith 1978). RUSLE developers recommend that slope length be measured from samples taken in the field or from topographic maps. However, measuring slope length or determining slope length from a map can be subjective (Renard et al. 1997). Moreover, it is a problem to measure slope length when the topography is complex and irregular (Desmet and Govers 1996), or to select “representative” transects in a farm field (Busacca et al. 1993).

The equation proposed by RUSLE developers (Renard et al. 1997) for calculating L is

$$L = (\lambda / 72.6)^m \quad (1)$$

where λ is the measured slope length, 72.6 is the RUSLE unit plot length in ft, and m is the

slope length exponent. The exponent m is related to the ratio β of rill erosion (caused by flow) to interrill erosion (principally caused by raindrop impact) by the following equation:

$$m = \beta / (1 + \beta) \quad (2)$$

When the soil is susceptible to both rill and interrill erosion, β can be computed from

$$\beta = (\sin \theta / 0.0896) / (3.0(\sin \theta)^{0.8} + 0.56) \quad (3)$$

where θ is the slope angle.

The equations for calculating S are:

$$S = 10.8 \sin \theta + 0.03, \text{ for slopes of less than } 9\% \quad (4)$$

$$S = 16.8 \sin \theta - 0.50, \text{ for slopes of } 9\% \text{ or steeper} \quad (5)$$

Both L and S also need to be adjusted for special conditions, such as the adjustment of the slope length exponent m for the erosion of thawing, cultivated soils by surface flow and the use of a different equation than (1) for slopes shorter than 15 feet. Usually L and S are combined into a single topographic factor LS , which represents the ratio of soil loss on a given slope length (L) and steepness (S) to soil loss from a slope that has a length of 72.6 ft and a steepness of 9%. The procedure for converting L and S into the LS factor varies, depending on if the slope is uniform, irregular, or segmented (Renard et al. 1997).

Moore and Burch (1986) have proposed a method for estimating LS for general use. Based on the unit stream power theory, the method uses the equation:

$$LS = (A_s / 22.13)^m (\sin \beta / 0.0896)^n \quad (6)$$

where A_s is the upslope contributing area per unit contour width, β is the slope angle, m is the slope length exponent, and n is the slope steepness exponent. The exponent m is estimated to be 0.6, and n 1.3. Several subsequent studies have assumed that the LS relationship in

Equation (6) is equivalent to the relationship in RUSLE (Moore and Burch 1986, Moore and Wilson 1992, Moore et al.1993, Moore and Wilson 1994, Gertner et al., 2002). However, McCool et al. (1993) have found that the slope length and steepness relationships derived from data from the humid regions of the United States tend to overestimate water erosion in the Northwestern wheat and range region. To account for regional topographic characteristics, McCool and his colleagues have proposed the following equations:

$$LS = (\lambda/22.13)^{0.5} (\sin \theta / 0.0896)^{0.6}, \text{ for slopes of 9\% or steeper} \quad (7)$$

$$LS = (\lambda/22.13)^{0.5} (10.8 \sin \theta + 0.03), \text{ for slopes of less than 9\%} \quad (8)$$

where λ is the horizontal slope length in meters, and θ is the slope angle in degrees.

The main difference between Moore and Burch (1986) and McCool et al. (1993) lies in the slope steepness exponent n , which is estimated to be 1.3 in Equation (6) and 0.6 in Equation (7). The two relationships also differ slightly in estimating the slope length exponent m .

USLE and RUSLE have evolved over the past 50 years. This soil erosion model has gone through numerous cycles of model development, calibration, and validation. The process continues.

3.2. WEPP

WEPP (Water Erosion Prediction Project), which is expected to replace RUSLE, is a process-based computer model for predicting soil erosion and sediment delivery on hillslopes and watersheds (Lafren et al. 1997). WEPP includes the three processes of soil erosion: detachment, transport, and deposition. The quantification of these processes occurs in the

erosion component in WEPP (Laflen et al. 1991). WEPP allows both spatial and temporal estimates of erosion and deposition on watershed consisting of hillslopes and channels (Flanagan and Livingston 1995).

The major inputs to WEPP are a climate data file, a slope data file, a soil data file, and a cropping/management data file. The climate file can be built using the CLIGEN program, either within the WEPP interface or outside of it, and the user has the option to choose from over 1000 weather stations in the United States. The slope file can be built either within the slope file builder interface, or by other means, such as in a GIS. The soil file can also be created through use of the soil file builder in the WEPP interface, or through use of a text editor. The cropping/management input file contains a number of different types of input parameters, which describe the different plants, tillage implements, forest conditions, management practices, etc. (Flanagan and Livingston 1995).

The WEPP model hillslope application requires information about the landscape geometry, which is entered by way of the slope input file. Required information includes slope orientation, slope length, and slope steepness at points down the profile (Flanagan and Livingston 1995). The WEPP hillslope model does not have a slope length and slope gradient factor as in USLE or RUSLE. Instead, the slope gradient and length inputs of WEPP are deeply integrated into the hydrology and erosion compliments of the model (Flanagan and Nearing 1995). This means that the measurements of slope length and slope gradient are not limited to affecting L and S factors as in USLE and RUSLE, but instead affect the calculations of runoff, friction, transport capacity, and various other factors, which eventually affect the prediction of erosion (Cochrane 1999).

The WEPP watershed model is an extension of the hillslope model that is applicable to small watersheds (less than 260 ha). It can be used to estimate watershed runoff and sediment yield. It assumes that watershed sediment yield is a result of detachment, transport, and deposition of sediment on overland (rill and interrill) flow areas and channel flow areas; in other words, it is a result of erosion from both hillslope areas and concentrated flow channels. In watershed applications, detachment of soil in a channel is predicted to occur if the channel flow shear stress exceeds a critical value and the sediment load in the flow is below the sediment transport capacity. Deposition is predicted to occur if channel sediment load is above the flow sediment transport capacity (Flanagan and Livingston 1995).

The three main components of the WEPP watershed model are hillslopes, channels, and impoundments. Additional files are required to describe the watershed configuration (the structure file), the channel topography (the channel slope file), the channel soils (the channel soil file), the channel management practices (the channel management file), and the channel hydraulic characteristics (the channel file) (Flanagan and Livingston 1995). The application of WEPP to a watershed requires that hillslopes be delineated and channels identified. Each hillslope, which is represented as a rectangle in WEPP, must have a representative length (L), width (W), and slope profile as shown in Figure 15. Hillslopes drain into the top, left side, or right side of a channel, eventually leading to the watershed outlet (Cochrane and Flanagan 2003).

4. TOPAZ

TOPAZ can preprocess a DEM by rectifying depressions and flat surfaces, identify hydrographic segmentations such as the channel network and corresponding drainage

divides, and calculate WEPP's topographic input parameters such as representative subcatchment parameters. The DEM processing in TOPAZ is based on the D8 flow routing method, and the critical source area (CSA) concept. The D8 flow routing method, as was discussed in the previous section, defines the drainage and flow direction on the landscape surface as the steepest downslope path from the cell of interest to one of its 8 adjacent cells. The CSA concept controls the watershed segmentation and all resulting spatial and topographic drainage network and subcatchment characteristics (Garbrecht and Martz 1999).

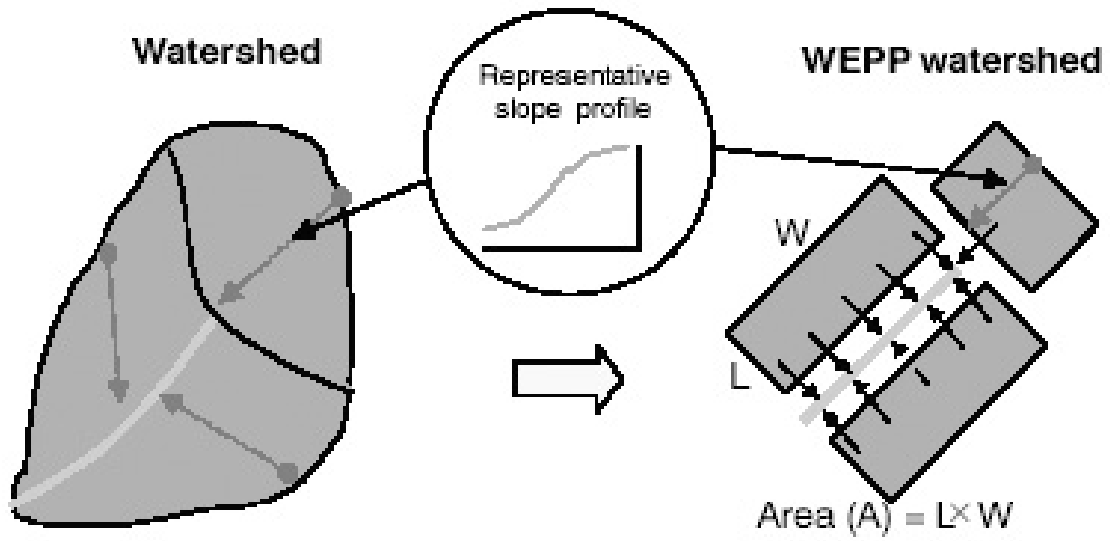


Figure 15. Watershed discretization for WEPP application (Cochrane and Flanagan 2003)

5. References

ArcDoc, *ArcGIS Help Documents*, (ESRI 2001).

Busacca, A.J., Cook, C.A., and Mulla, D.J., 1993, Comparing landscape-scale estimation of soil erosion in the Palouse using Cs-137 and RUSLE. *Journal of Soil and Water Conservation*, **48**, pp. 361-367.

Cochrane, T.A., 1999, Methodologies for watershed modeling with GIS and DEMs for the parameterization of the WEPP model. Ph.D. thesis, Purdue University.

Cochrane, T.A., and Flanagan, D.C., 2003, Representative hillslope methods for applying the WEPP model with DEMs and GIS. *Transactions of the ASAE*, **46**(4), pp. 1041-1049.

Costa-Cabral, M.C., and Burges, S.J., 1994, Digital elevation model networks (DEMON): a model of flow over hillslopes for computation of contributing and dispersal areas. *Water Resources Research*, **30**, pp. 1681-1692.

Desmet, P.J.J., and Govers, G., 1996, A GIS-procedure for automatically calculating the USLE LS factor on topographically complex landscape units. *Journal of Soil and Water Conservation*, **51**(5), pp. 427-433.

Endreny, T.A., and Wood, E.F., 2003, Maximizing spatial congruence of observed and DEM-delineated overland flow networks. *International Journal of Geographical Information Science*, **17**, pp. 699–713.

Fairfield, J., and Leymarie, P., 1991, Drainage networks from grid digital elevation models. *Water Resources Research*, **27** (5), pp. 709-717.

Flanagan, D.C., and Livingston, S.J., 1995, WEPP user summary, USDA-Water Erosion Prediction Project (WEPP). (W. Lafayette, IN: USDA-ARS National Soil Erosion Research Laboratory).

Flangan, D.C., and Nearing, M.A., 1995, Technical documentation, USDA-Water erosion Prediction Project (WEPP). *NSERL Report*, **10**, (USDS-ARS National Soil Erosion Research Laboratory, West Lafayette, IN).

Florinsky, I.V., 1998, Accuracy of local topographic variables derived from digital elevation models. *International Journal of Geographical Information Systems*, **12**, pp. 47–61.

Foster, G.R., 1982, Modeling the erosion process. In *Hydrologic Modeling of Small Watershed*. C.T. Haan, H.P. Johnson, and D.L. Brakensiek (Ed.), An ASAE monograph number 5 in a series published by American Society of Agricultural Engineers.

Garbrecht, J., and Martz, L.W., 1999. TOPAZ Overview. Rep.# GRL99-1, Grazinglands Research Laboratory, USDA ARS, April 1999, El Reno, Oklahoma.

Garbrecht, J., and Martz, L.W., 2000, Digital elevation model issues in water resources modeling. In *Hydrologic and Hydraulic Modeling Support with Geographic Information Systems*. D. Maidment, and D. Djokic (Ed.), (Redland, CA: ESRI Press).

Gertner, G., Wang, G., Fang, S., and Anderson, A.B., 2002, Effect and uncertainty of digital elevation model spatial resolution on predicting the topographical factor for soil loss estimation. *Journal of Soil and Water Conservation*, **57**(3), pp. 164-174.

Hutchinson, M. F., 1989, A new procedure for gridding elevation and stream line data with automatic removal of spurious pits. *Journal of Hydrology*. **106**, pp. 211-232.

Hutchinson, M.F., 1996, A locally adaptive approach to the interpolation of digital elevation models. *The Proceedings of Third International Conference/Workshop on Integrating GIS and Environmental Modeling*, January 21-26, 1996, Santa Fe, NM.

Jenson, S.K., and Domingue, J.O., 1988, Extracting topographic structure from digital elevation data for geographic information system analysis. *Photogrammetric Engineering and Remote Sensing*, **54**, pp. 1593-1600.

Laflen, J.M., Lane, L.J., and Foster, G.R., 1991, WEPP: a new generation of erosion prediction technology. *Journal of Soil and Water Conservation*, **46**, pp. 34-38.

Laflen, J.M., Elliot, W.J., Flanagan, D.C., Meyer, C.R., and Nearing, M.A., 1997, WEPP – predicting water erosion using a process-based model. *Journal of Soil and Water Conservation*, **52**(2), pp. 96-102.

Lea, N.L., 1992, An aspect driven kinematic routing algorithm. In *Overland Flow: Hydraulics and Erosion Mechanics*, A.J. Parsons and A.D. Abrahams (Ed.) pp. 393–407 (New York: Chapman and Hall).

Luce, C.H., 1995, Forests and wetlands, In *Environmental Hydrology*, A.D. Ward, W.J. Elliot (Ed.), CRC Lewis Publishers, pp. 253-284.

Mark, D.M., 1983, Automated detection of drainage networks for digital elevation models, *Proceedings of Auto-Carto*, **6**(2), Ottawa, Ontario, Canada, pp. 288-298.

McCool, D.K., George, G.O., Freckleton, F., Douglas, C.L., Papendick, Jr., R.I., 1993, Topographic Effect on Erosion from Cropland in the Northwestern Wheat Region. *American Society of Agricultural Engineers*, **36**(4), pp. 1067-1071.

Mitasova, H., and Iverson, L.R., 1996, Erosion and sedimentation potential analysis for Hunter Lake. In *An environmental assessment of the Hunter Lake project area*, W.U.

Brigham, and A.R. Brigham (Ed.) pp. 1.2.01 – 1.2.08. (Champaign: Illinois Natural History Survey),

Moore, I.D., and Burch, G.J., 1986, Physical basis of the length-slope factor in the Universal Soil Loss Equation. *Soil Science Society of America Journal*, **50**, pp. 1294-1298.

Moore, I.D., Grayson, R.B., and Ladson, A.R., 1991, Digital terrain modeling: a review of hydrological, geomorphological, and biological applications. *Hydrological Processes*, **5**, pp. 3-30.

Moore, I.D., Turner A.K., Wilson, J.P., Jenson, S.K., and Band, L.E., 1993, GIS and land-surface-subsurface process modelling. In *Environmental Modeling with GIS*, M.F. Goodchild, B.O. Park, and L.T. Styært (Ed.), pp. 213–230 (Oxford, UK: Oxford University Press).

Moore, I.D., and Wilson, J.P., 1992, Length-slope factor for the Revised Universal Soil Loss Equation: simplified method of estimation. *Journal of Soil and Water Conservation*, **47**, pp. 423-428.

Moore, I.D., and Wilson, J.P., 1994, Reply to comments by foster on “Length-slope factor for the Revised Universal Soil Loss Equation: simplified method of estimation.” *Journal of Soil and Water Conservation*, **49**, pp.174-180.

O’Callaghan, J.F., and Mark, D.M., 1984, The extraction of drainage networks from digital elevation data. *Computer Vision, Graphics and Image Processing*, **28**, pp. 328-344.

Reid, L.M., 1993, Research and cumulative watershed effects. USDA Forest Service, Pacific Southwest Research Station, General Technical Report GTR-141, pp.118.

Renard, K.G., Foster, G.R., Weesies, G.A., McCool, D.K., and Yoder, D.C., 1997, Predicting soil erosion by water: a guide to conservation planning with the revised Universal Soil Loss Equation (RUSLE). *Agricultural Handbook 703*, Washington, DC: U.S. Department of Agriculture.

Tarboton, D.G., 1997, A new method for the determination of flow directions and upslope areas in grid digital elevation models. *Water Resources Research* **33**(2), pp. 309-319.

USGS <http://ned.usgs.gov/Ned/faq.asp> USGS NED Frequently Asked Questions. (accessed 15 March 2005).

Wilson, J.P., and Gallant, J.C., 2000, *Terrain Analysis: Principles and Applications*. (John Wiley & Sons, Inc).

Zhou, Q., and Liu, X., 2002, Error assessment of grid-based flow routing algorithms used in hydrological models. *International Journal of Geographic Information Science*, **16**(8.), pp. 819-842.

Appendix B

Statistical programs and outputs

1. The SAS code and output for the ANOVA test of the watershed area, runoff, and sediment yield of watersheds 5 and 6.

```

DATA A;
INFILE 'D:\Data\GeoWEPPRuns\Results\SAS\Wboth.PRN';
INPUT METHOD $ AREA RUNOFF EROSION WTSD $;
PROC PRINT;
PROC ANOVA;
CLASS METHOD WTSD;
MODEL AREA = WTSD METHOD;
RUN;
PROC ANOVA;
CLASS METHOD WTSD;
MODEL RUNOFF = WTSD METHOD;
RUN;
PROC ANOVA;
CLASS METHOD WTSD;
MODEL EROSION = WTSD METHOD;
RUN;

```

Obs	METHOD	AREA	RUNOFF	EROSION	WTSD
1	OBS	176.60	406500	4.55	W6
2	OBS	106.43	138940	1.38	W5
3	L30	178.27	375795	6.20	W6
4	L30	112.94	241118	5.60	W5
5	N30	176.14	374452	6.20	W6
6	N30	110.72	238844	4.00	W5
7	S30	175.96	362753	9.60	W6
8	S30	112.31	235007	14.10	W5
9	L10	176.56	378949	4.30	W6
10	L10	106.06	227102	2.10	W5
11	N10	179.62	371966	6.20	W6
12	N10	111.66	232654	2.50	W5
13	L4	176.83	383005	3.90	W6
14	L4	107.26	229098	2.20	W5

The ANOVA Procedure

Class Level Information

Class	Levels	Values
METHOD	7	L10 L30 L4 N10 N30 OBS S30
WTSD	2	W6 W5

Number of observations 14

The ANOVA Procedure

Dependent Variable: AREA

Source	DF	Sum of Squares	Mean Square	F Value	Pr > F
Model	7	15993.97780	2284.85397	616.39	<.0001
Error	6	22.24089	3.70681		
Corrected Total	13	16016.21869			

R-Square	Coeff Var	Root MSE	AREA Mean
0.998611	1.342775	1.925309	143.3829

Source	DF	Anova SS	Mean Square	F Value	Pr > F
WTSD	1	15953.62571	15953.62571	4303.86	<.0001
METHOD	6	40.35209	6.72535	1.81	0.2435

The ANOVA Procedure

Class Level Information

Class	Levels	Values
METHOD	7	L10 L30 L4 N10 N30 OBS S30
WTSD	2	W6 W5

Number of observations 14

The ANOVA Procedure

Dependent Variable: RUNOFF

Source	DF	Sum of Squares	Mean Square	F Value	Pr > F
Model	7	89934857438	12847836777	10.73	0.0051
Error	6	7182408638	1197068106		
Corrected Total	13	97117266075			

R-Square	Coeff Var	Root MSE	RUNOFF Mean
0.926044	11.54338	34598.67	299727.4

Source	DF	Anova SS	Mean Square	F Value	Pr > F
WTSD	1	88111355118	88111355118	73.61	0.0001
METHOD	6	1823502320	303917053	0.25	0.9402

The ANOVA Procedure

Class Level Information

Class	Levels	Values
METHOD	7	L10 L30 L4 N10 N30 OBS S30
WTSD	2	W6 W5

Number of observations 14

The ANOVA Procedure

Dependent Variable: EROSION

Source	DF	Sum of Squares	Mean Square	F Value	Pr > F
Model	7	124.0014500	17.7144929	4.71	0.0389
Error	6	22.5833857	3.7638976		
Corrected Total	13	146.5848357			

R-Square	Coeff Var	Root MSE	EROSION Mean
0.845936	37.29380	1.940077	5.202143

Source	DF	Anova SS	Mean Square	F Value	Pr > F
WTSD	1	5.8760643	5.8760643	1.56	0.2580
METHOD	6	118.1253857	19.6875643	5.23	0.0320

2. The SAS code and output for the ANOVA test of the slope values derived from the six DEMs.

```
DATA B;
INFILE 'D:\Data\GeoWEPPRuns\Results\SAS\Slope.PRN';
INPUT METHOD $ SLP PNT $;
PROC PRINT;
PROC ANOVA;
CLASS METHOD PNT;
MODEL SLP = PNT METHOD;
RUN;
```

Obs	METHOD	SLP	PNT	Obs	METHOD	SLP	PNT
1	L30	6.28	p1	7	L30	14.66	p7
2	L30	7.30	p2	8	L30	14.99	p8
3	L30	7.54	p3	9	L30	15.28	p9
4	L30	10.28	p4	10	L30	15.37	p10
5	L30	10.88	p5	11	L30	17.20	p11
6	L30	13.95	p6	12	L30	17.34	p12

Obs	METHOD	SLP	PNT	Obs	METHOD	SLP	PNT
13	L30	18.53	p13	80	S30	19.41	p20
14	L30	18.58	p14	81	S30	19.54	p21
15	L30	19.13	p15	82	S30	19.68	p22
16	L30	19.17	p16	83	S30	20.27	p23
17	L30	19.69	p17	84	S30	20.50	p24
18	L30	20.06	p18	85	S30	20.60	p25
19	L30	20.13	p19	86	S30	20.78	p26
20	L30	20.25	p20	87	S30	21.89	p27
21	L30	20.77	p21	88	S30	22.28	p28
22	L30	20.88	p22	89	S30	27.62	p29
23	L30	20.88	p23	90	S30	28.03	p30
24	L30	21.15	p24	91	L10	3.92	p1
25	L30	21.70	p25	92	L10	4.78	p2
26	L30	21.96	p26	93	L10	5.43	p3
27	L30	22.00	p27	94	L10	11.20	p4
28	L30	23.81	p28	95	L10	12.21	p5
29	L30	24.12	p29	96	L10	13.61	p6
30	L30	27.03	p30	97	L10	14.12	p7
31	N30	6.40	p1	98	L10	16.30	p8
32	N30	7.55	p2	99	L10	16.49	p9
33	N30	8.52	p3	100	L10	17.07	p10
34	N30	9.98	p4	101	L10	17.69	p11
35	N30	12.65	p5	102	L10	18.50	p12
36	N30	12.89	p6	103	L10	18.55	p13
37	N30	12.98	p7	104	L10	18.71	p14
38	N30	14.11	p8	105	L10	19.74	p15
39	N30	15.05	p9	106	L10	19.98	p16
40	N30	15.60	p10	107	L10	21.84	p17
41	N30	15.68	p11	108	L10	22.34	p18
42	N30	16.57	p12	109	L10	23.26	p19
43	N30	16.84	p13	110	L10	24.66	p20
44	N30	17.21	p14	111	L10	25.60	p21
45	N30	17.45	p15	112	L10	26.52	p22
46	N30	17.86	p16	113	L10	26.86	p23
47	N30	17.87	p17	114	L10	27.39	p24
48	N30	17.90	p18	115	L10	27.54	p25
49	N30	18.53	p19	116	L10	28.76	p26
50	N30	19.52	p20	117	L10	28.80	p27
51	N30	20.00	p21	118	L10	29.33	p28
52	N30	20.18	p22	119	L10	30.23	p29
53	N30	20.59	p23	120	L10	32.56	p30
54	N30	22.71	p24	121	N10	2.11	p1
55	N30	23.29	p25	122	N10	7.32	p2
56	N30	24.07	p26	123	N10	7.98	p3
57	N30	26.97	p27	124	N10	11.05	p4
58	N30	27.71	p28	125	N10	12.05	p5
59	N30	29.50	p29	126	N10	13.21	p6
60	N30	30.16	p30	127	N10	13.56	p7
61	S30	4.76	p1	128	N10	13.95	p8
62	S30	7.43	p2	129	N10	16.08	p9
63	S30	7.58	p3	130	N10	16.29	p10
64	S30	8.29	p4	131	N10	17.34	p11
65	S30	10.67	p5	132	N10	17.83	p12
66	S30	11.09	p6	133	N10	17.95	p13
67	S30	11.33	p7	134	N10	18.02	p14
68	S30	11.67	p8	135	N10	18.83	p15
69	S30	11.74	p9	136	N10	20.07	p16
70	S30	12.11	p10	137	N10	21.08	p17
71	S30	12.61	p11	138	N10	21.14	p18
72	S30	14.05	p12	139	N10	21.56	p19
73	S30	16.61	p13	140	N10	22.10	p20
74	S30	17.20	p14	141	N10	22.22	p21
75	S30	17.45	p15	142	N10	22.60	p22
76	S30	17.72	p16	143	N10	22.97	p23
77	S30	17.83	p17	144	N10	24.06	p24
78	S30	18.40	p18	145	N10	24.36	p25
79	S30	19.20	p19	146	N10	28.50	p26

Obs	METHOD	SLP	PNT	Obs	METHOD	SLP	PNT
147	N10	30.22	p27	164	L4	19.93	p14
148	N10	30.30	p28	165	L4	19.94	p15
149	N10	30.54	p29	166	L4	20.11	p16
150	N10	36.73	p30	167	L4	21.19	p17
151	L4	3.09	p1	168	L4	23.58	p18
152	L4	5.01	p2	169	L4	23.76	p19
153	L4	6.03	p3	170	L4	24.61	p20
154	L4	9.88	p4	171	L4	24.86	p21
155	L4	10.43	p5	172	L4	25.69	p22
156	L4	10.86	p6	173	L4	25.81	p23
157	L4	14.00	p7	174	L4	28.16	p24
158	L4	16.52	p8	175	L4	31.01	p25
159	L4	17.58	p9	176	L4	31.44	p26
160	L4	17.59	p10	177	L4	31.73	p27
161	L4	19.25	p11	178	L4	34.04	p28
162	L4	19.32	p12	179	L4	37.43	p29
163	L4	19.58	p13	180	L4	38.05	p30

The ANOVA Procedure

Class Level Information

Class	Levels	Values
METHOD	6	L10 L30 L4 N10 N30 S30
PNT	30	p1 p10 p11 p12 p13 p14 p15 p16 p17 p18 p19 p2 p20 p21 p22 p23 p24 p25 p26 p27 p28 p29 p3 p30 p4 p5 p6 p7 p8 p9

Number of Observations Read 180

Number of Observations Used 180

The ANOVA Procedure

Dependent Variable: SLP

Source	DF	Sum of Squares	Mean Square	F Value	Pr > F
Model	34	8610.311202	253.244447	70.79	<.0001
Error	145	518.714229	3.577340		
Corrected Total	179	9129.025431			

R-Square	Coeff Var	Root MSE	SLP Mean
0.943180	10.09612	1.891386	18.73378

Source	DF	Anova SS	Mean Square	F Value	Pr > F
PNT	29	8146.834898	280.925341	78.53	<.0001
METHOD	5	463.476304	92.695261	25.91	<.0001